



Hydrothermal mineralising systems as chemical reactors: Wavelet analysis, multifractals and correlations

Alison Ord ^{a,*}, Mark Munro ^a, Bruce Hobbs ^{a,b}

^a Centre for Exploration Targeting, University of Western Australia, WA 6009, Australia

^b CSIRO, Perth, WA 6102, Australia



ARTICLE INFO

Article history:

Received 11 December 2015

Received in revised form 17 March 2016

Accepted 18 March 2016

Available online 25 April 2016

ABSTRACT

Hydrothermal mineralising systems are discussed as large, open flow chemical reactors held far from equilibrium during their life-time by deformation and the influx of heat, fluid and dissolved chemical species. As such they are nonlinear dynamical systems and need to be analysed using the tools that have been developed for such systems. Hydrothermal systems undergo a number of phase transitions during their evolution and this paper focuses on methods for characterising these transitions in a quantitative manner and establishing whether they resemble either abrupt or continuous (critical) phase transitions or whether they have some other kind of nature. Critical phase transitions are characterised by long range correlations for some parameter characteristic of the system, power-law probability distributions, so that there is no characteristic length scale, and a high sensitivity to perturbations. The transitions undergone in mineralised hydrothermal systems are: (i) widespread, non-localised mineral alteration involving exothermic mineral reactions that produce hydrous silicate phases, carbonates and iron-oxides, (ii) strongly localised veining, brecciation and/or stock-work formation, (iii) a series of localised endothermic mineral reactions involving the formation of non-hydrous silicates, sulphides and metals such as gold, (iv) multiple overprinting repetitions of transitions (ii) and (iii). We quantify aspects of these transitions in some gold deposits from the Yilgarn craton of Western Australia using wavelet transforms. This technique is convenient and fast. It enables one to establish if the transition is multifractal (and if so, quantify the multifractal, or singularity, spectrum) and to determine the scale dependence of long range correlations or anti-correlations. Other aspects of the spectrum enable quantitative distinctions between sub-critical, critical and super-critical systems. The availability of long drill holes with detailed chemical analyses and mineral abundances derived from hyperspectral data enables individual ore bodies to be characterised rapidly in a quantitative manner and constraints placed on whether the various transitions are possibly critical or of some other form. We also present some simple nonlinear models, including numerical simulation, self-organised branching and multiplicative cascade processes that produce the multifractal character and correlation scaling relations observed in these data sets. Distinctions between systems that are strongly and weakly mineralised are discussed.

© 2016 Published by Elsevier B.V.

1. Introduction and statement of the problem

The formation of hydrothermal systems, and their associated patterns of rock alteration, veining, brecciation and mineralisation, presents one of the most scientifically challenging parts of the geosciences. These systems are examples of the ultimate in full coupling between mechanical, hydrological, thermal and chemical processes and operate as highly nonlinear entities. An understanding of the processes involved in the formation of these systems is of fundamental economic importance in a world that has a continuing demand for metals in a scientific and industrial environment where discovery rates are declining and the cost of discovery is increasing. For over 100 years scientific

investigations of hydrothermal systems have been directed at studies of individual mineral deposits at ever increasing detail but still with no unified view of what controls the location, size and grade of individual deposits. More recently (Occhipinti et al., 2016) the discipline has adopted a systems approach where the mineral deposit is viewed as part of an integrated crustal or lithospheric scale system in which a number of processes associated with fluid production, transport and mixing and metal deposition are considered together. Still the fundamental principles and parameters that define location, size and grade have not emerged in any coherent manner. For the most part, the traditional view of mineralising systems has been grounded in concepts associated with linear system behaviour, a view that is embedded in the conceptually and mechanically unrealistic *source-transport-trap* concept of mineral systems. The outstanding example of linear system behaviour is an assumption that chemical equilibrium thermodynamics controls what we see.

* Corresponding author.

E-mail address: alison.ord@uwa.edu.au (A. Ord).

We present the view that hydrothermal mineralising systems are archetypal, large, nonlinear, non-equilibrium, evolving systems in which a number of interacting parts and processes result in highly irregular spatial and temporal distributions of alteration mineral assemblages, of deformation such as fracturing, veins and breccias, at a number of scales, and of mineralisation and sulphides. The evolution of these systems involves a number of phase transitions such as unaltered → altered, undeformed → brecciated, and un-mineralised → mineralised. These features are some of the hallmarks of systems that are now widely studied under the umbrella of *Nonlinear Dynamical Systems*, a subject that has evolved significantly over the last 120 years since the pioneering works of Poincaré (1892); Gibbs (1902; *Dover rendition*, 1960); Lotka (1910, 1920); Onsager (1944); Prigogine (1955); Lorenz (1963) and Mandelbrot (1974). The literature associated with Nonlinear Dynamical Systems is now too large to adequately review or summarise here and much new material is emerging each month particularly in the fields of non-equilibrium critical systems and pattern formation in very large non-equilibrium systems (Cross and Greenside, 2009).

Hydrothermal mineralised systems are *stochastic* in nature. By this we mean that they exhibit great irregularity in the spatial distributions of alteration mineral assemblages, mineral chemistry, mineralisation, fracturing, veining and brecciation. The term *stochastic* is used to mean that probability distributions need to be used to describe such spatial distributions rather than simple mathematical relations. The basic question we ask is: Are these stochastic distributions the result of chance where the concentration of one mineral or the density of veining or of brecciation is unrelated to a neighbouring one? Or is the apparent irregularity the result of an underlying deterministic process that produces patterns that are apparently stochastic but are intrinsically deterministic? If the latter is true, then spatial correlations in alteration, mineralisation and veining/brecciation should exist and one might expect that large, high grade mineral deposits are characterised by long range correlations. Moreover, processes operating at a range of spatial scales from lithospheric plumbing system scales to the nano-metre chemical reaction scale promote interactions and correlations at an array of spatial scales. Hence one expects the resultant signatures in hydrothermal systems to scale in different ways at different spatial scales and hence to be multifractal in nature.

We consider hydrothermal mineralising systems as large open flow chemical reactors held far from chemical equilibrium by flows of heat, fluids and chemical components. At the same time mechanical disequilibrium is maintained by the flow of momentum, expressed as veining and brecciation. Closed chemical systems must always evolve (Ross, 2008, p4) to an equilibrium state (which is itself a stationary state where no evolution of the system occurs) whereas open flow systems can evolve to one or more non-equilibrium stationary states and remain there, or switch from one non-equilibrium state to another, for as long as the flows are maintained (Ord et al., 2012). These are characteristics of nonlinear dynamical systems.

The tantalising question is: What processes generate a large, high grade mineral deposit as opposed to a small disseminated deposit? In keeping with our view of mineralising systems as chemical reactors we propose that the following conditions need to be met to generate a large high grade deposit:

- Processes and geometries for efficient fluid mixing must exist.
- A plumbing system exists such that as much as possible of the reactive material in the system can be accessed. This means that optimal fluid and heat flow geometries must be developed that do not involve channelling of fluids into a small number of conduits.
- Within the system, intimate access to nutrients must exist.
- Large contact areas between reactants and nutrients must be generated during the fluid mixing process. This means that although the flow might remain laminar a pore or fracture geometry exists that enables chaotic flow to develop (Ottino, 1994; Lester et al., 2012). We emphasise that the term *chaotic* in this sense does not necessarily

imply turbulent flow (Hobbs and Ord, 2015, pp 390–393).

- The shape and size of the system has to optimise heat loss so that maximum possible yield results (Aris, 1961).

These are the conditions that a chemical engineer would take into account in designing an efficient high yielding chemical reactor. In addition a chemical engineer would need to optimise the net present value (NPV) of the reactor cost given other constraints imposed upon her. Luckily we do not need to consider such monetary issues but perhaps mother Nature does. Perhaps She (being intrinsically a thermodynamicist) requires that the equivalent of NPV (entropy production) is maximised given the constraints on the system (which may for instance be pre-existing crustal structure)? Or perhaps She requires that the configuration of the plumbing system maximises entropy? These are overarching, fundamental issues regarding hydrothermal systems that need to be addressed in the future.

One way of expressing the criteria for producing a high yielding mineralising reactor is that of Bejan and Lorente (2008) in the form of their *Constructal Law* which they claim is a fundamental law of Nature: *for a finite-size flow system to persist in time (to live) it must evolve such that it provides greater and greater access to the currents that flow through it*. Although this seems to be an excellent description of the plumbing system that must develop in order to optimise fluid and heat transport in a high yielding mineralising system it does not address some of the other dot points mentioned above. It does however imply that we should be able to observe long range spatial correlations in the patterns of alteration, mineralisation and deformation we see in mineralised systems. We return to the *Constructal Law* in the discussion.

Another way of tackling the question is to explore the system of mathematical equations that would describe the operation of mineralising systems and see if we can distil from these some useful basic principles that enable us to understand these systems a little better. The operation of a chemical reactor is described by a set of mathematical equations that cover the dot points mentioned above. These equations (see Appendix A) are fully coupled to each other and describe the following processes. By *fully coupled* we mean that each process has a first order feedback on all of the other processes.

- Mass balance.
- Heat transfer.
- Fluid transport including the coupled mechanics of permeability generation and destruction.
- Chemical reaction kinetics including the *chemical* mechanisms of permeability generation and destruction.
- Mechanical deformation including the *mechanical* mechanisms of permeability generation and destruction.

In keeping with a large number of natural nonlinear dynamical systems the solutions to these equations are invariably chaotic (Aris, 1978; Lynch et al., 1982; Gray and Scott, 1994; Burghardt and Berezowski, 1996; Berezowski, 2000; Berezowski, 2014; Berezowski et al., 2000) and because of the very large number of thermodynamic states generated by chaotic behaviour (Beck and Schlogl, 1993) the systems are intrinsically *multifractal*. Just as the concept of *entropy* arises in statistical mechanics (Sethna, 2011) from any physical system because of the very large number of atomic states the concept of a *multifractal singularity spectrum* arises in chaotic systems because of the very large number of chaotic states (Beck and Schlogl, 1993).

A multifractal in our context is a geometrical pattern made up of a number of spatially intertwined fractals each with its own fractal dimension. An additional characteristic feature of such systems is that their evolution is punctuated by a series of phase transitions where the system changes its qualitative behaviour (Sethna, 2011). At these phase transitions long range correlations develop where the system has no intrinsic length scale (in other words, the correlations are

fractal). Phase transitions are termed *critical transitions* if they possess long range correlations. If the system continuously evolves so that it remains critical over extended periods of time, or repeatedly cycles through criticality, the behaviour is termed *self-organised criticality*.

It is important therefore in regarding mineralising systems as nonlinear dynamical systems to analyse the features that we observe in such systems using the concepts and techniques that have been developed for other nonlinear dynamical systems over the past 50 years or so. Thus the questions we would ask of mineralising systems are: (i) Is the distribution of alteration mineral assemblages, mineral chemistry, mineralisation and structure (such as veining and brecciation) fractal? We know from cursory observations that these distributions are stochastic, but is there any quantifiable regularity in such distributions? (ii) If the distribution of alteration, chemistry, mineralisation and structure is fractal can we go further and enquire if these distributions are multifractal? This means that different parts of the spatial distribution scale differently with respect to spatial dimensions. (iii) Are there any spatial correlations to be revealed in these stochastic data sets? Are there short or long range correlations and, if so, over what length scales? The answers to these questions are important because long range

correlations are the hall-mark of critical systems whereas short range correlations are typical of systems approaching criticality. (iv) Can we use the knowledge of multifractal geometry and the presence or absence of spatial correlations to say something concerning the mechanisms of formation of mineral systems?

To place this paper in context and give some motivation we present in Fig. 1 some data sets from hydrothermal systems. Fig. 1 (a and b) show abundances of chlorite and gold measured along diamond drill-holes in a mineralised system in the Yilgarn of Western Australia. The chlorite data set resembles at least superficially the plots for deterministic systems we will explore in Section 3. The gold data resemble more an intermittent signal that one might see in a turbulent fluid (Frisch, 1995, Chapter 8) or the energy release in an earthquake sequence (inset Fig. 1b). The questions we ask here are: *Do these signals represent the response of a critical system? Are the signals fractal or even multifractal? Or are they something else? Is there some kind of systematic behaviour in these signals that reflects the nonlinear dynamics of the system?*

In Fig. 1 (c and d) we show behaviour where the fractal dimension of regional scale “complexity” has been mapped in Fig. 1 (c) and correlated

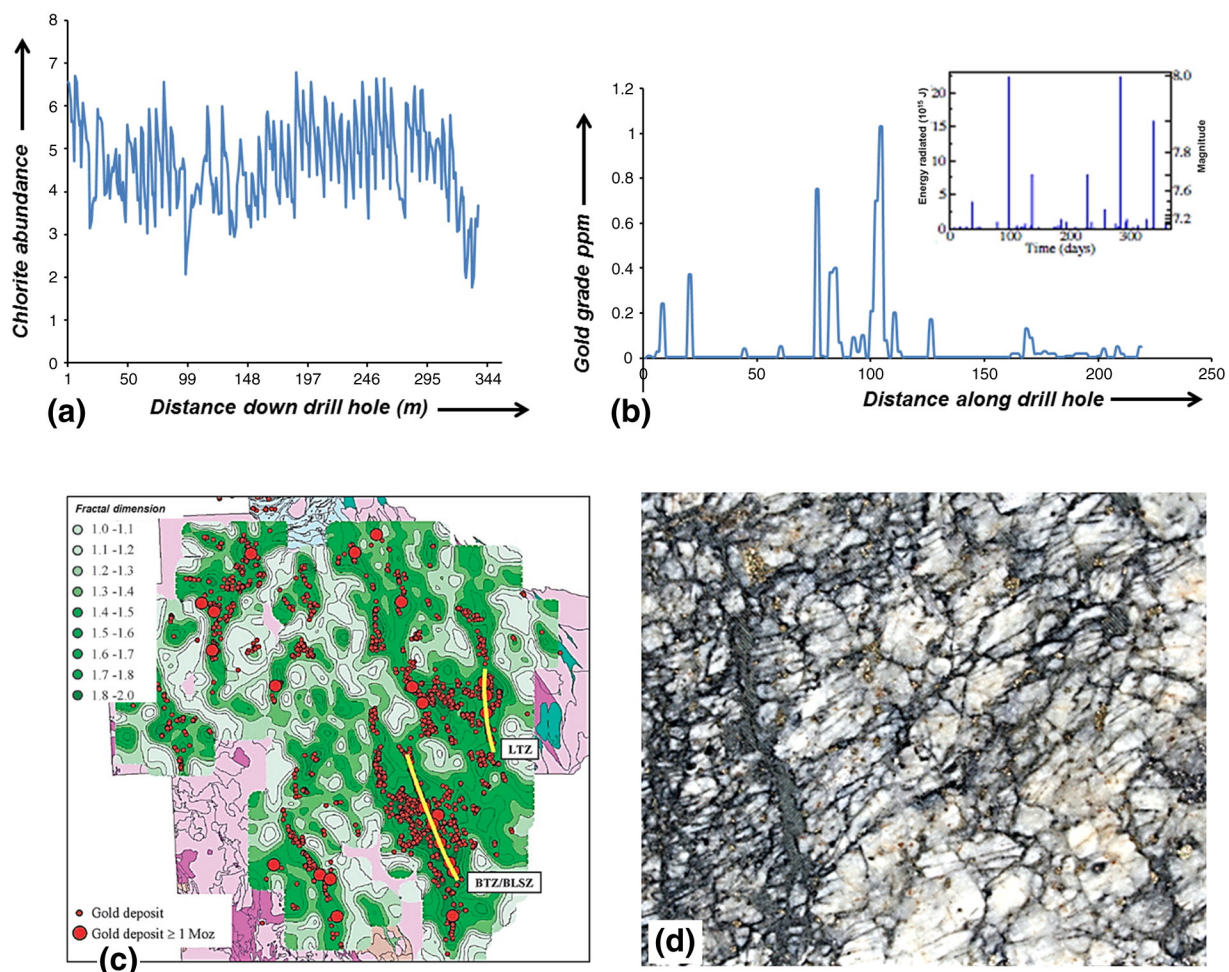


Fig. 1. Data sets from hydrothermal systems. (a) Chlorite abundance (Mineral abundance is measured in various ways in practice and in this paper. Sometimes, as in this figure, the abundance is a multiple of the sum of abundances of all other minerals measured. In Fig. 15(a) it is the proportion of that mineral in the total rock to the abundance of all the minerals measured. At other times as in Figs. 8(c), 10(a), 11(a) and 12(a) it is the number of pixels containing that mineral measured in the core at a sampling point. We always use the raw data as supplied by the mining company. Since the wavelet analysis is sensitive to the relative values of fluctuations in the data the measure of abundance is not important for our purposes.) along a drill hole measured by infra-red reflectance methods. Salt Creek gold deposit, Western Australia. Inset: energy release sequence for earthquakes in California, 1995. (c) Map of “complexity” in part of the Yilgarn craton of Western Australia. The figure is a contoured map of fractal dimension (determined by box counting) of mapped structures with gold occurrences superimposed. Yellow lines show locations of the Bardoc Tectonic Zone and Boulder – Lefroy Shear Zone (BTZ/BLSZ) in the Kalgoorlie Terrane and the Laverton Tectonic Zone (LTZ). After Hodkiewicz et al. (2005). See that paper for details. (d) Image of fractures in a breccia from the Tropicana gold deposit in Western Australia. Bright golden specs are gold bearing arseno-pyrite grains. Scale: Image is 1.5 cm across base.

with gold occurrence whilst in Fig. 1 (d) the distribution of fractures at the hand specimen scale is shown in a breccia from the Tropicana deposit in Western Australia. We want to know the answers to the above questions for these data sets.

In order to address these various issues we need a rapid way of analysing the vast data sets that are now available from many ore bodies. Such data sets include hyperspectral determinations of mineral abundances, multi-element chemical analyses, assays for gold and detailed structural data sets on vein/fracture orientations and distributions. We propose the wavelet transform as a means of analysis to extract the multifractal (or singularity) spectrum using the Wavelet Transform Maximum Modulus (WTMM) formalism (Arneodo et al., 1995). This paper, to a large extent, is meant as an introduction to and use of the WTMM formalism. We also examine spatial correlations using the Hurst exponent (Feder, 1988; Arneodo et al., 2002, 2003; Sprott, 2003) corresponding to the wavelet transform at a number of spatial scales.

This paper is concerned with answers to the various questions posed above and is structured as follows. In Section 2 we examine the concept of phase transitions in hydrothermal systems and in particular the associated concepts of criticality and of self-organised criticality. Section 3 is devoted to deterministic versus stochastic behaviour and to the dynamics of cascade processes whilst Section 4 considers the multifractal formalism together with methods of establishing spatial correlations. Section 5 presents some examples from Yilgarn gold deposits in Western Australia. Section 6 discusses some models that produce the types of patterns observed in mineralised systems; section 7 concludes the paper. We defer detailed mathematical concepts to the two appendices. The paper is mainly concerned with some of the techniques involved in analysing hydrothermal systems and illustrating these techniques with some examples from mineralising systems. Future papers will present in depth analyses of individual mineral deposits.

2. Critical systems and self-organised criticality

A new paradigm for understanding hydrothermal mineralising systems is built around the following five propositions:

- Hydrothermal systems are open flow chemical reactors that remain far from equilibrium in mechanical, hydrological, thermal and chemical terms for as long as nutrients and energy are fed to the system. The size and grade of any deposit is a function of the time that its associated system remains open and the efficiency (reflected in the nature of spatial correlations in the system) of the networked processes that operated within the reactor. The open flow nature of the systems coupled with feedback relations between chemical-mechanical-hydrological-thermal processes leads to system behaviour that is chaotic where the term chaotic is used to indicate that the system behaviour is sensitive to initial conditions. Thus no two ore systems are identical; they show irregular distributions of structure, alteration and mineralisation and preserve a paragenetic sequence. Yet these systems are the product of deterministic processes. These are all the hallmarks of non-equilibrium, chaotic systems.
- In keeping with systems held far from equilibrium by external forcing (deformation gradients, fluid pressure gradients, thermal gradients, and chemical potential gradients) hydrothermal mineralising systems are characterised by the competition between processes that produce heat and those that consume energy. These include exothermic processes that dissipate energy (the production of hydrous silicates such as sericite, biotite and chlorite, precipitation of iron oxides, quartz and carbonates together with brecciation) and endothermic processes that consume energy (precipitation of sulphides and metals, dissolution of quartz to form stylolites). The optimal operation of the system corresponds to one or more non-equilibrium stationary states where the energy exchange between these competing

processes balances. Such stationary states may or may not be stable (Aris, 1999). Many examples for open flow chemical reactors are given by Gray and Scott (1994).

- Hydrothermal systems are critical systems where the term *critical* is meant in the classical sense of the word and not necessarily in the sense of *self-organised criticality*. This means that a critical system is one that undergoes one or more phase transitions where a homogeneous, structure-less system develops structure at a number of spatial and temporal scales with well-defined scaling laws and where intermittency and long range correlations exist (Sethna, 2011). The problem in such systems is to understand these scaling laws and the physical-chemical processes responsible for them.
- Since these systems are open throughout their life the model: *source-transport-trap* gives an incorrect conceptual view of the evolution of such systems and thus provides concepts that can be misleading. Thus the idea that domes or anticlinal hinges provide concentration sites for fluids is completely misleading in an over-pressured system with a fluid pressure gradient greater than hydrostatic and with the hydrological constraint of continuous fluid flow (Hobbs and Ord, 2015, pp 386–388). A better analogue would be with a chemical reactor such as an internal combustion engine where the system of interest is described by: *fuel tank(s)-fuel line(s)-reaction site-exhaust system* (Fig. 2).
- The sources for alteration fluids (*the fuel tanks*) are far better constrained than perhaps 5 years ago. The thermodynamic constraints on sources of CO₂, K-rich and Na-rich fluids within the lithosphere are also much better defined now and provide clear exploration concepts that enable more precise questions to be asked (Gonzalez et al., 2015). We explore these issues in a subsequent paper.

Even though system behaviour is chaotic, well defined procedures exist to describe, characterise and analyse such systems. These procedures are grounded in the physics and chemistry of the processes that operate and are inherently more robust and useful from an exploration sense than existing empirical, pattern recognition or statistical procedures.

2.1. Self-organised criticality. Threshold dynamics

The concept of criticality has been made popular by Bak (1996) who proposed that some systems, when gently forced from an equilibrium state, ultimately reach a threshold where some kind of scale independent phenomenon emerges and persists. This phenomenon was christened *self-organised criticality* by Bak and co-workers (Bak et al., 1987). The archetype example proposed was the slow loading of a sand-pile until a scale independent pattern of avalanches emerges. This behaviour (the best examples of which appear in computer experiments and not in natural systems) was proposed as one example of critical behaviour although the precise physics behind the process has never been enunciated. Experimental examples of self-organised criticality have been reported from piles of specially elongate rice grains.

The concept called *self-organised criticality* is given some detailed discussion by Sornette (2006). He gives the following criteria for self-organised criticality:

- The system is driven at a constant very slow rate and composed of many interacting components.
- The system has highly nonlinear behaviour with essentially a threshold response.
- The threshold corresponds to a globally stationary state, characterised by a stationary probability distribution.
- These probability distributions are power-law in nature with fractal geometries and long-range correlations.

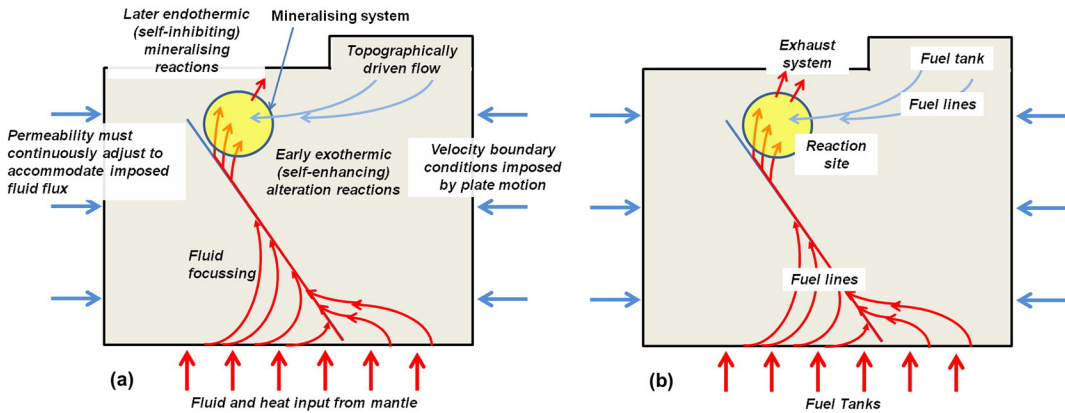


Fig. 2. The geometry of a hydrothermal mineralising system. (a) A crustal model showing mantle derived fluids focussed into a crustal scale fault system and fluids leaving the fault in the hanging wall to react with topographically driven fluids. (b) The same system as (a) with fuel tanks, fuel lines, reaction site and exhaust system marked. The principles governing the focussing process are discussed in Zhao et al. (2008, 2009).

The problem with the use of the term *self-organised criticality* (SOC) is that the concept is loosely defined and there is a temptation to use the term because it tends to give the system the responsibility and ability to organise itself and hence commonly implies there is no further need for explanation. As indicated above, Sornette (2006) has offered some criteria that characterise SOC but no mechanisms based in physics or chemistry are offered. The issue is that all of the four criteria offered by Sornette can arise from other processes including abrupt phase changes (non-critical), second order phase changes (critical) and many phenomena associated with bifurcation (non-critical). One could ask the following questions that embrace the hallmarks of criticality: *Is SOC like a continuous phase transition that involves the evolution of heterogeneities described by scaling exponents? Does SOC involve a loss in convexity for an energy function? Does SOC involve the minimisation of an energy function? SOC clearly is a non-equilibrium phenomenon so is the stationary state mentioned in Sornette's list a super-critical state? How would I distinguish a SOC system from one undergoing a first or continuous transition?* As far as we are aware there are no clear answers to these questions which is why the concept is so loosely defined. Due to the lack of constraints on the concept an SOC system can behave in any manner the proponent wishes (subject to Sornette's list). In a way, SOC systems resemble the concept of mantle plumes which can also behave in any way the proponent wishes. One should read the paper by Lundin (2013): *Plumes do that*. The sentiments expressed by Lundin are directly applicable to the SOC concept as it is presently defined and applied.

However the concept of SOC does imply that the system is held at criticality for an extended period of time or continuously evolves through one or more critical states. As an example of a model in which the system continuously revisits criticality we consider one developed by Lyakhovsky and Ben-Zion (2008). This is an example of the type of analysis that needs to be developed for hydrothermal systems. The theory begins with the definition of the Helmholtz energy for a damaging solid where damage is defined as any process (brittle or viscous) that degrades the load bearing capacity of the material. The Helmholtz energy as defined encompasses the energy arising from the classical linear Hooke's law but is modified by the addition of an energy term that describes the opening and closing of cracks; this results in nonlinear elasticity. The form of this definition needs to take into account that the elastic moduli depend on the nature of the deformation, particularly that the elastic moduli in tension degrade more rapidly than in compression (Lockner and Byerlee, 1980). From this energy the nonlinear constitutive equation for an elastic-viscous material with cracks may be derived. A restriction imposed by the second law of thermodynamics, namely that the entropy production must always be

greater or equal to zero, is used to derive a thermodynamically admissible evolution law for subsequent damage. Instability is defined by a loss in convexity of the Helmholtz energy; this can coincide with a bifurcation where the governing equations lose ellipticity (Rudnicki and Rice, 1975) but in general the two criteria for instability do not coincide and in this instance loss of convexity precedes loss of ellipticity. Finally the post-failure evolution is modelled using evolution laws that involve the healing of damage. The result is illustrated in Fig. 3 where the system first evolves slowly as damage begins to accumulate and then faster until criticality, defined by loss of convexity, is reached. The system then relaxes until some healing process begins (such as precipitation of quartz). The healing process reduces the damage so that the whole process repeats. Thus the system continuously cycles through criticality as a series of avalanches.

Another model for SOC is that of self-organised branching (Zapperi et al., 1995) which we return to in Section 6. Yet other models we will return to and that are not based on the SOC concept are various cascade models (Chainais, 2006; Ihlen and Vereijken, 2010) that have long been used in the analysis of mineralised systems (de Wijs, 1951, 1953; Turcotte, 1986; Agterberg, 2007; Cheng, 2008; Ford and Blenkinsop, 2009). Instead of the concept of SOC we prefer models for the evolution

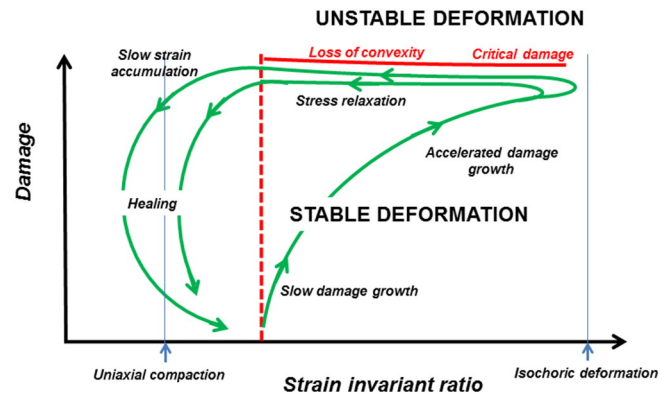


Fig. 3. The earthquake cycle as modelled by a non-local form of the energy involving diffusion and healing of damage. From Lyakhovsky et al. (2011). The system first evolves towards an isochoric deformation as damage slowly accumulates and damage density diffuses through the system. Damage growth accelerates and at a critical value of the damage the system "loses convexity" and becomes unstable. At this stage the stresses relax. Healing then sets in and the system begins to deform slowly again undergoing uniaxial compaction. The process then repeats, the result being continuous revisiting of a critical state.

of hydrothermal mineralising systems based on principles to do with minimisation of the energy of the system as in the Lyakhovsky model.

From this point of view the behaviours discussed above can be summarised as follows. Many aspects of deformation can be described as first-order (or abrupt) phase transitions. However instead of the phase changes being sharp as in classical, ideal first-order transitions the ones of interest are extended over a broader range of driving parameters (such as stress or strain) and they show hysteresis which is manifest as different behaviours under different loading conditions. These behaviours arise because the energy barriers involved (regions of increased strength or elastic moduli) are large in magnitude compared to thermal fluctuations and are of relatively large spatial extent. Instead of the energy landscape being smooth with just two minima as in a classical abrupt or continuous phase transition (Fig. 4a) the energy landscape is rugged and consists of numerous local minima (Fig. 4b); the energy barriers are such that thermal fluctuations play a negligible role. The system can only move from one energy-well to another through the external driving force. This means that thermal fluctuations alone are not enough to drive the phase transition and high levels of stress or of strain are necessary. The high energy barriers have two origins: (i) initial (quenched) disorder that is inherited from a former state; these determine initial nucleation sites for the new phase; (ii) new microstructure such as fracture surfaces and damage zones which are spatially localised. This means that the response of the material to a constant driving force is a series of nucleation and collective de-pinning events expressed as discontinuous jumps, as local high strength regions are overcome and neighbouring regions take up the stress, followed by periods of quiescence when propagation of the advancing phase boundary is pinned. The next avalanche is associated with de-pinning of this boundary and this de-pinning event is expressed as an avalanche of damage events.

An important aspect of such avalanche behaviour is that spatial patterns of damage or of enhanced chemical reaction tend to develop. Mathematically, pattern formation is a difficult process to treat (Cross and Greenside, 2009). In the simplest of nonlinear systems the energy function has two basins as shown in Fig. 4 (a) which means that there are two stable solutions to the equations that describe pattern formation and the resulting pattern consists of a regular array of spots or stripes. However for most cases the equations involved constitute a system of coupled nonlinear equations that may be impossible to solve analytically with current mathematical tools or sometimes the equations can be shown to have an indefinite number of solutions. The system hops from

one solution to another as it evolves; each solution corresponds to a basin within a rugged energy topography such as is illustrated in Fig. 4 (b). A common approach is to make some assumptions that hopefully are realistic physically and chemically in order to make the equations involved linear. It is then possible to perturb the system by a small amount and analyse whether the perturbed state is stable (returns to its unperturbed state) or is unstable (grows into a pattern). In nonlinear systems such a solution is only valid for the conditions where the initial linearization assumptions hold. One cannot make predictions about the pattern after these assumptions break down and commonly the system switches to another state at that stage. The initial growth rates predicted by the linear analysis (which are commonly exponential) slow down once the nonlinear effects start to dominate (Cross and Greenside, 2009, pp 129–139). Generally computer simulation is the only way to proceed but even there sensitivity to initial conditions and to the boundary conditions may lead to solutions that are not general. One should be aware of these issues in examining claims made in the literature.

3. Deterministic versus stochastic behaviour

The well-known irregularity exhibited by mineralised systems may result from purely random events (as described by the tossing of a coin) or there may be an underlying origin that appears stochastic yet contains important embedded information. The problem is to distinguish between these two possibilities. The classical linear approach to the behaviour of systems is that they are either *deterministic* or *stochastic*. The term *deterministic* is meant to imply that if one knows the initial conditions of the system and the ways in which the boundary conditions have changed with time then the behaviour of the system at some future time can be predicted. *Stochastic* implies that processes operating during the evolution of the system interact in a random manner so that the final outcome of the interactions can only be predicted in terms of probabilities.

The fundamental question that needs to be answered in gaining an understanding of hydrothermal mineralising systems is:

Given that the behaviour of hydrothermal systems is governed by a series of deterministic equations (those that describe deformation, chemical reactions and heat and fluid flow), why are such systems characterised by apparently stochastic spatial distributions of deformation, alteration and mineralisation?

Poincaré (1892) was the first to show that even a small number of interacting nonlinear processes (in his case, three) can result in

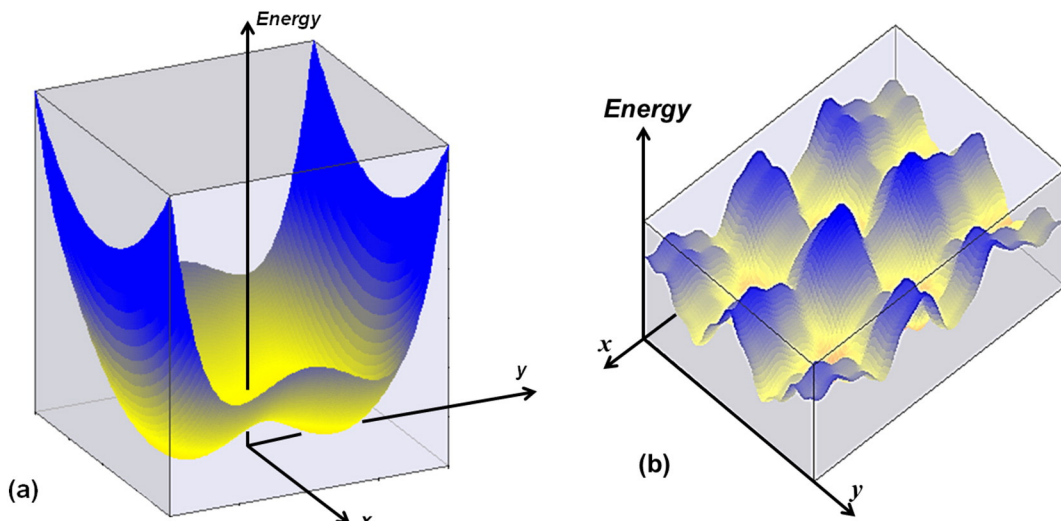


Fig. 4. Energy configurations as a function of two variables, x and y , which could for instance be strain and fluid flow velocity. (a) A two-well energy potential representing two states where the energy is minimised. (b) A multi-well energy function where, as the system evolves, a number of local states are available to minimise the local energy function. The system evolves by jumping from one energy well to another. If the energy barriers are large compared to thermal fluctuations then *avalanche* behaviour is possible as the driving force overcomes a local barrier only to throw impediments to subsequent evolution of the system on to another nearby energy barrier which subsequently fails as a cascade. There are many studies of these kinds of systems; a summary is in Hobbs and Ord (2015, pp 223–234, 338–345).

irregular behaviour but his work was not widely embraced until perhaps the 1970's when it became accepted that for nonlinear systems (even very simple ones) irregular behaviour is the norm rather than an interesting exception. We, in the geosciences community, still need to make that transition, both in understanding and acceptance, with respect to most processes that take place in the lithosphere of the Earth.

A characteristic of many natural systems, such as the development of turbulence in fast flowing fluids, is that the driving forces that cause the system to evolve are imposed at a large length scale but the dissipative processes operate at smaller length scales. Thus in hydrothermal systems the driving forces may be imposed at length scales measured in thousands of kilometres whereas the dissipative processes may operate down to the nanometre scale. The interval between the scale where forcing occurs and the smallest dissipative scale, is called the *inertial interval*, or the *transparency window* (Frisch, 1995). For hydrothermal systems the inertial interval covers at least 15 orders of magnitude.

In natural nonlinear systems where the forcing processes operate at a large length scale and the dissipative processes operate at smaller scales the energy transfer occurs across the scales by a *cascade* process whereby processes operating at large length scales shed energy to processes operating at smaller length scales until finally at small scales the dissipation is negligible or processes (such as endothermic mineral reactions) operate that consume energy. This process is expressed in the famous poem by Richardson (1922) regarding turbulent flow in the atmosphere:

Big whirls have little whirls
Which feed on their velocity,
And little whirls have lesser whirls
And so on to viscosity.

In general the cascade process in hydrothermal systems is towards smaller length scales so that large ore bodies are always associated spatially with a cascade of ever smaller mineralised packages. Such a cascade process to smaller and smaller length scales is called a *direct cascade* and one example is cataclasis or brecciation where both mass and energy are transferred to smaller and smaller scales by a crushing or fracturing process. Lightning is another example of a direct cascade; the distributed accumulation of electrons at a cloud's surface during a thunderstorm ultimately results in a downward cascade of electrons into the ground with progressive fingering of the discharge downwards; the process can be described in terms of multifractals (Gou et al., 2007; Faghfouri, 2011). For mineralised hydrothermal systems one might write, paraphrasing Richardson:

Big ore bodies have little ore bodies
The result of criticality,
And little bodies have lesser bodies
And so to multifractality.

We develop the details associated with this ditty throughout this paper. In Fig. 5 (a) the mineralised packages are shown as regular geometrical features and the same geometry is repeated at smaller length scales so that the system is self-similar. Clearly this is not the case in

nature and considerable irregularity in spatial distribution is generally observed as presented in Fig. 5 (b). In some systems such as turbulent fluid flow this irregularity is called *intermittency*. Intermittency is a characteristic of most naturally occurring systems and is best developed in mineralised systems in the spatial distribution of mineralisation (at all scales).

However cascade processes can operate from small to larger scales in some natural systems. This is called an *inverse cascade* and a natural example is the agglomeration of water drops to form a cloud or the agglomeration of rain drops on a window pane to form a rivulet. Another example is the case of metamorphic systems where the progressive agglomeration of partial melt ultimately forms a pluton. Here both energy (in the form of latent heat) and mass are cascaded to larger and larger scales. A very similar example of an indirect cascade is the formation of a large hydrothermal mineralised system where fluxes of heat and fluids are progressively focussed into a single highly reactive site (Fig. 2) where metals are concentrated to levels up to 10^4 above background levels. With apologies to Richardson:

Small concentrations grow to big concentrations
That feed on energy advection,
Big concentrations grow to larger concentrations
And so to explorers' satisfaction.

In view of the extreme spatial and temporal irregularity commonly observed in hydrothermal ore bodies, highly relevant questions are: Is all this irregularity purely random? Or do these systems follow some kinds of rules? And is it possible to make some sense out of all the irregularity? In anticipation of the remainder of this paper the answers to these questions are no, yes and yes, but we need to develop some new tools in order to discover the beauty in the systematics inherent in this behaviour.

In order to give some feel for the answers to these questions we look at a very simple system that has many of the irregular characteristics of mineralising systems. We view hydrothermal systems as dynamical systems (those that evolve with time) and, as such, distinguish two end-member types of dynamical systems. One is a deterministic system in which the future state of the system is determined by the nature of some previous state according to some mathematical formula. The other is a stochastic system where the future state of the system is defined by some random process such as the toss of a coin. We consider hydrothermal systems to be governed by the laws inherent in the behaviour of physical and chemical systems and hence are deterministic dynamical systems. Such systems show a variety of behaviours and can exhibit chaotic behaviour (that is, sensitivity to initial conditions) if the mathematical relations involved in defining the evolution of the system are nonlinear.

One characteristic of the evolution of hydrothermal systems is that they can be considered to be iterative systems. That is, the state of the system at one instant depends on the immediately previous state in time. An example is the evolution of permeability where the permeability at one instant depends on the value in a previous instant. An

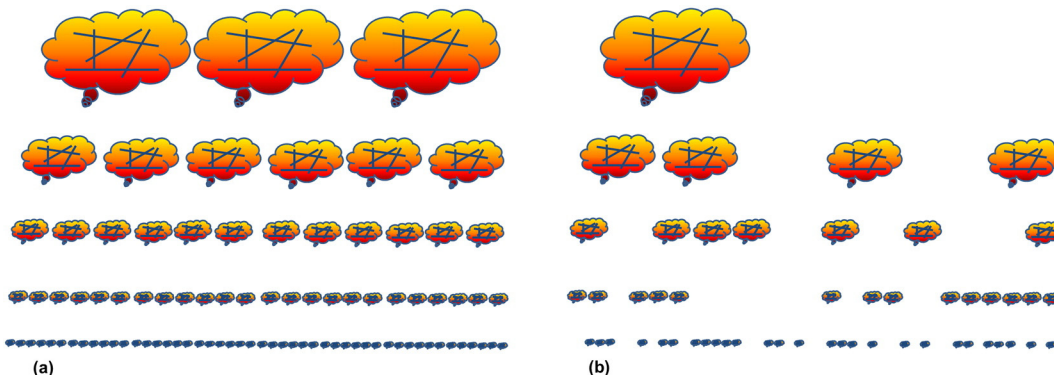


Fig. 5. Fractal size distribution of ore bodies. (a) A fractal self-similar distribution. (b) A fractal distribution with intermittency. Intermittency is characteristic of gold distributions at all scales from the nano-meter to regional scales.

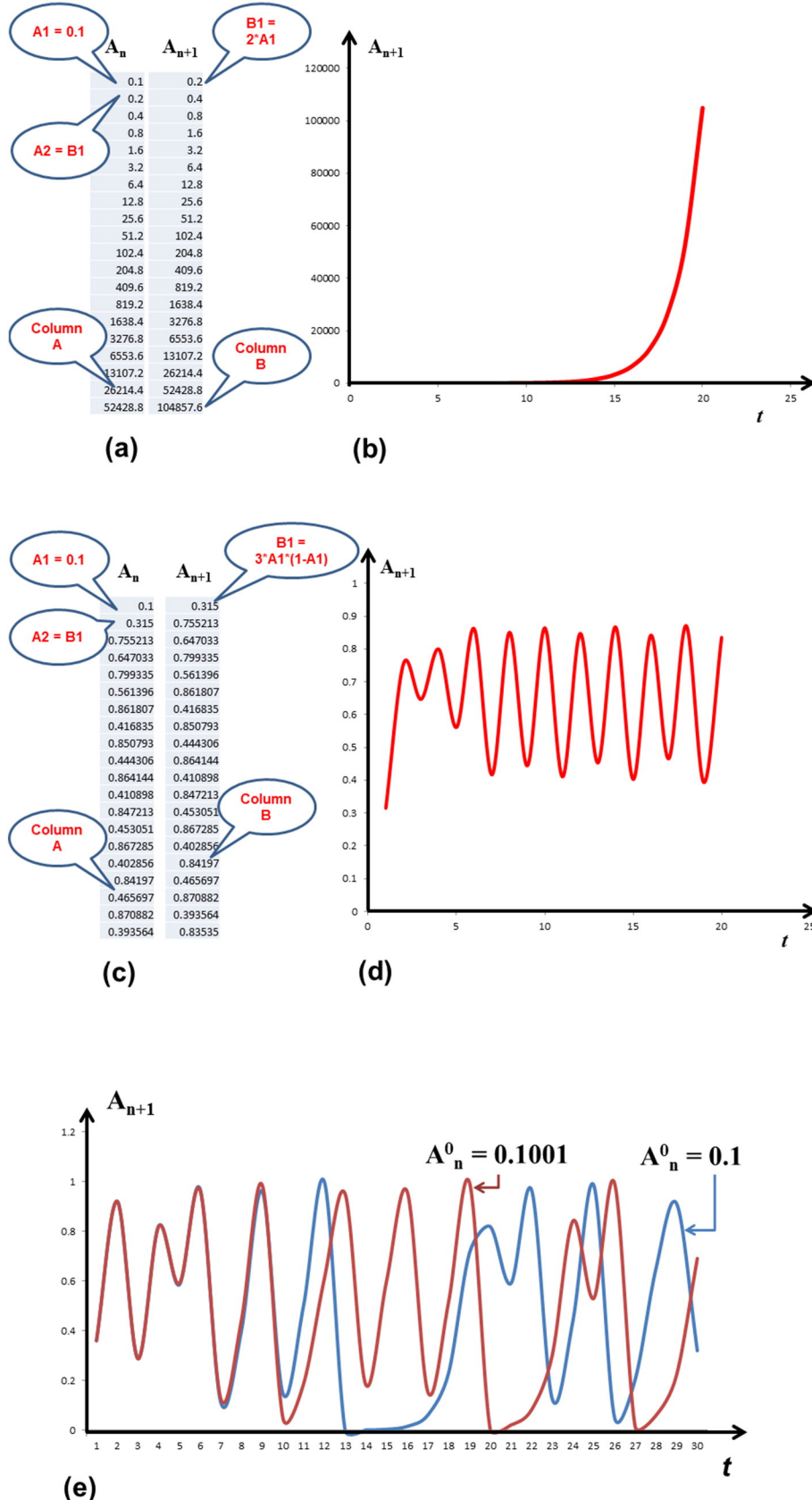


Fig. 6. Some aspects of iterative behaviour. (a) A system with no competition to growth given by (1). This represents the two columns A and B of a spreadsheet with the formulae entered to calculate the iterations described by (1). The result is exponential growth as shown in (b). (c) The spreadsheet for the iterative scheme given in (2) with $\alpha = 3$ and the initial value of $A = 0.1$. (d) The behaviour of the iterative scheme with time. The response is close to periodic with two wavelengths of similar amplitude. (e) The behaviour of (2) with $\alpha = 4.0$. For the blue curve the initial value of A is 0.1000; for the brown curve the initial value of A is 0.1001. This figure demonstrates the sensitivity of the system to initial conditions. (f) Intermittent (burst or clumping) behaviour of the logistic system over the first 250 steps with $A_0 = 0.2$ and $\alpha = 3.8$. (g) Return map for data in (f). (h) Return map for data in (i). (i) Random numbers between 0 and 1 generated using Random Number Generator in Excel.

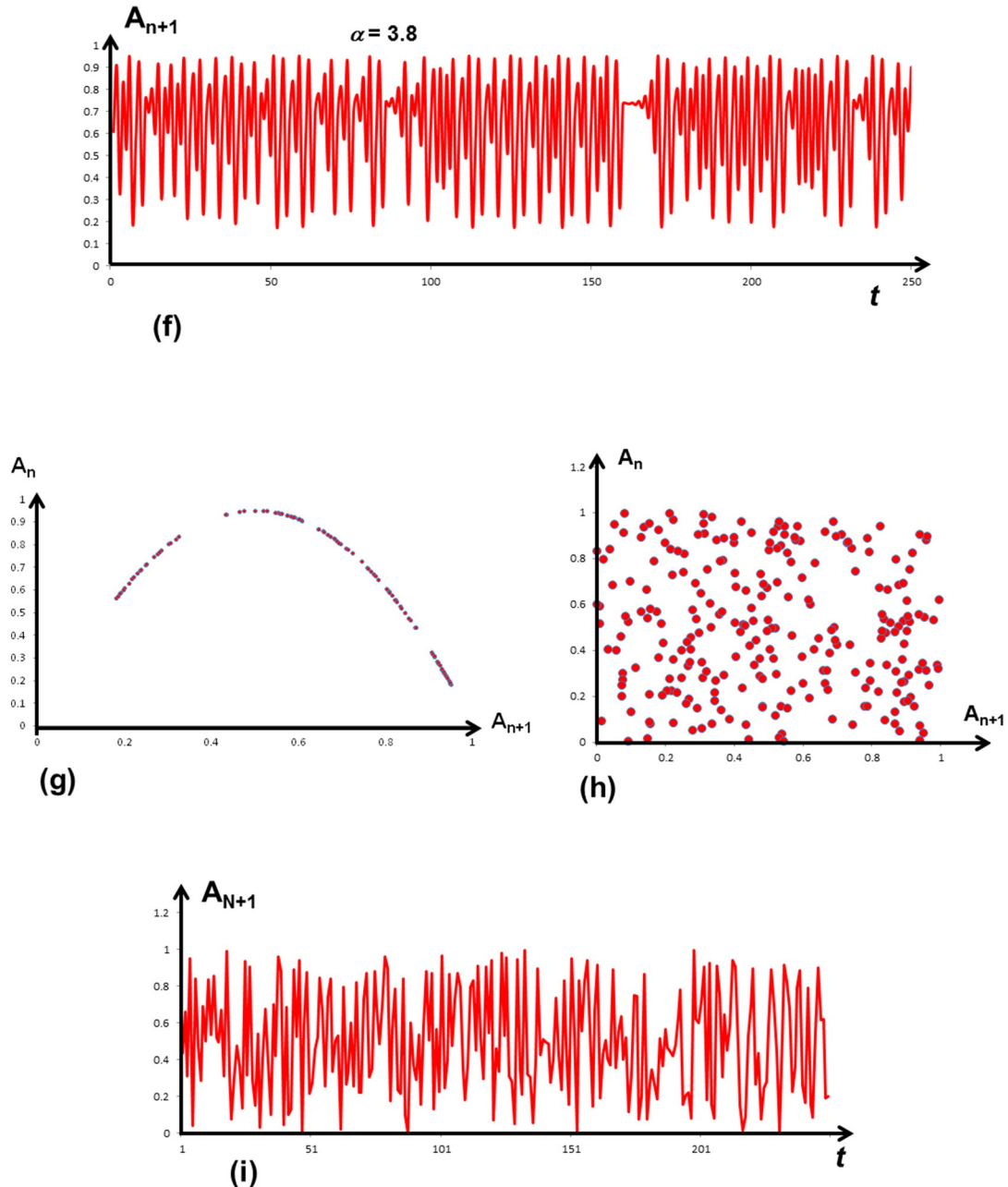


Fig. 6 (continued).

additional characteristic is that this dependency on a previous state may depend on other processes that operate in the system so that there is feedback between different simultaneous processes. We first consider a system where there is no feedback and the value of some quantity, such as the concentration of some species, A , at time $t = n + 1$, A_{n+1} , depends solely (in a linear manner) on the concentration at time $t = n$:

$$A_{n+1} = \alpha A_n \quad (1)$$

where α is a constant. Expressions such as (1) are an example of a discrete dynamical system and such relations are useful in trying to understand complex systems where the real mathematical equations are difficult or perhaps impossible, to solve. If we assume for example that $\alpha = 2$ and start with, say $A_n = 0.1$, then we can calculate A_{n+1} at all

future times using an Excel spreadsheet. The first 20 entries in this evolution are shown in Fig. 6 (a) and plotted in Fig. 6 (b).

Fig. 6 (a and b) represents a system that grows with no competition and depends only on its previous state; it simply grows exponentially. However, as we have seen in Section 2, the characteristic feature of systems not at equilibrium is competition between processes. So, let us now write an expression that embodies competition;

$$A_{n+1} = \alpha A_n (1 - A_n). \quad (2)$$

The first part of the right hand side of this expression, αA_n , expresses exponential growth as we have seen. The second part, $-\alpha A_n^2$, expresses the fact that some of A is being used in a nonlinear manner in another process (such as another mineral reaction) so now there is competition for the growth of A . Now if we run our spreadsheet, with $\alpha = 3$, we get

Fig. 6 (c and d). The system now evolves to periodic behaviour with two slightly different wavelengths present.

If we now increase α to 4 still with the initial value of $A = 0.1$ we obtain the blue curve in **Fig. 6** (e) where the first 30 steps are plotted. The resulting behaviour is now non-periodic and in fact is quite irregular. Some might call the behaviour random but in fact the behaviour is clearly deterministic since we can easily say what the behaviour will be between say steps 1000 and 1030 by running our Excel spreadsheet.

There is an additional fundamental aspect to the behaviour of this system for $\alpha = 4$. If we change the initial value of A by 0.1% from 0.1000 to 0.1001 and run our spreadsheet again, we obtain the brown curve in **Fig. 6** (e). This duplicates the behaviour of the system for the first 5 or so steps but then begins to diverge so that by 30 steps there appears to be no correlation in behaviour even though both the blue and red curves are completely deterministic. This sensitivity to initial conditions is formally known as *chaos*. Sensitivity to initial conditions is also demonstrated by changing α in Eq. (2) by a small amount. As an exercise, **Fig. 6** (f) results for $\alpha = 3.8$. As a spectacular exercise the reader should decrease α by 13.6% and try $\alpha = 3.284$.

The simple system described by Eq. (2) exhibits one other important form of behaviour, *intermittency* with apparently irregular bursts of activity. If we run our spread sheet again with initial conditions $A_0 = 0.2$ and with $\alpha = 3.8$ we obtain **Fig. 6** (f) which displays intermittent behaviour. Further aspects of the behaviour of Eq. (2) which is called the *logistic equation* are considered by Sprott (2003).

Although the signal in **Fig. 6** (f) is irregular, one can extract fundamental information from the signal by a very simple construction called a *return map* (Sprott, 2003). We simply plot the value of the signal at $n = 1$ against the value at $n + 1$ and repeat the procedure. So the next point is obtained by plotting A_{n+1} against A_{n+2} and so on. The result is **Fig. 6** (g) which is the *attractor* for the signal in **Fig. 6** (f). This is none other than the plot of Eq. (2). Thus the underlying iterative process that produces the irregular signal in **Fig. 6** (f) can be extracted from the data by constructing a return map.

Notice, by zooming into **Fig. 6** (g), that the return map has structure within it. Thus the attractor for this system is fractal. A fractal attractor is called a *strange attractor*. The return map for a random signal shown in **Fig. 6** (i) is given in **Fig. 6** (h). The clear randomness of the signal is revealed by the return map.

These simple examples show that very simple nonlinear relations lead to chaotic behaviour including intermittency. In the next section we look at some ways of describing and analysing such deterministic chaotic behaviour.

4. Multifractal features of ore systems and spatial correlation

Many features of hydrothermal systems such as the spatial distribution of alteration, veining, brecciation and mineralisation are not only irregular but the same kind of irregularity is also expressed at a number of spatial scales. One way of investigating such irregularity at a wide range of spatial scales is to consider if the irregularity constitutes a *fractal geometry*. We use the term *fractal* to mean any geometrical object that has structure at all spatial scales such that when one looks at finer and finer scales one sees much the same kind of structure. For some fractals one has to homogeneously deform the small scale image to statistically reproduce the large scale view of the structure. Such a fractal is called a *self-similar* fractal.

Formally a *fractal* is an object that has structure at all length scales and some measure of this structure is invariant with respect to an affine transformation (Mandelbrot, 1982). This means that the object has structure within structure. From a mathematical point of view the way in which the structure scales with length is a power law:

$$P(\varepsilon) \approx \varepsilon^D \quad (3)$$

where $P(\varepsilon)$ is the probability that a part of the object lies within a box of size ε (examples are the presence of fractures or of gold within a box of size, ε); ε is a length scale and D is commonly known as the *fractal dimension*.

It is important in what follows to distinguish between simply noting whether some part of the object lies within a box of given size as opposed to noting the concentration or some *measure* of the object within that box. Examples are to note whether gold exists within a given box as opposed to noting the concentration of gold within that box or to note whether a vein exists in a box as opposed to noting the density of veins in that box. The first way of representing the image leads to the determination of the *fractal dimension* whereas noting the concentration or measure within each box leads to a determination of the *multiperiodic spectrum* (if it exists). In mathematical terms, a fractal is a set (or array of objects) whereas a multifractal can arise if one assigns values (or a *measure*) to each point in that set.

It should be appreciated that not all fractals are self-similar. *Self-similar fractals* remain the same under the influence of any transformation that is a *dilation* (a contraction or expansion of equal magnitude in all directions). The word *same* here is meant to imply that at different scales the pattern has identical statistical properties as measured say by the probability distribution (see Frisch, 1995, his Chapters 3 and 8). Fractals also exist that are *self-affine*; these are objects that remain the same under *affine transformations* other than a dilation (for instance, a homogeneous biaxial distortion). Thus a surface such as a fault plane appears smooth at a coarse length scale but is rough at a fine length scale. These surfaces are *self-affine fractals*. Scale invariance cannot continue indefinitely and so fractal geometries are practically restricted in hydrothermal systems to three to perhaps five or six orders of magnitude in length scales (corresponding say to scaling from 1 mm to 100 m or 1 km). There are other types of fractals, a common one in hydrothermal systems being an *intermittent fractal* (Frisch, 1995, Chapter 8). Here magnification of different parts of the fractal gives different results in that intermittent fractals show fractal behaviour for some parts of the system but not for others (**Fig. 6f**). Gold distributions are classical examples of intermittent fractals (**Fig. 1b**).

Fractals are *singular*¹ functions from a mathematical point of view since they cannot be differentiated and so D is also known as a *singularity measure*. The interesting feature of Eq. (3) is that D is commonly a non-integer. The reason that self-similar geometries follow a power law of the form (Eq. (3)) is that it is the only form of relation where changing the size of ε leaves the form of the equation unaltered. Thus if we double the size of ε we get

$$P(2\varepsilon) \approx (2\varepsilon)^D = 2^D \varepsilon^D. \quad (4)$$

The “box counting” method for determining D in Eq. (3) has been reviewed by Kruhl (2013) and is also considered by Feder (1988); Schroeder (1991) and Kruhl (1994). Applications to mineral systems are given by Arias et al. (2011); Bastrakov et al. (2007); Ford and Blenkinsop (2009); Hunt et al. (2007); Li et al. (2009); Oreskes and Einaudi (1990); Qingfei et al. (2008); Riedi (1998) and Sanderson et al. (2008). Fractal (or at least, power law) distributions of mineralisation are reported by Carlson (1991) and Schodde and Hronsky (2006). D is commonly known as the *box counting dimension*.

One should be aware of the pitfalls involved in fitting power laws to measured data sets and that a power law distribution established over a limited range of length scales does not necessarily imply fractal

¹ A singularity is some behaviour of a function that cannot be defined mathematically. This may mean, for instance, that the function is discontinuous, diverges to infinity or that it is not differentiable at a particular point.

geometry; this can be the situation, for instance, if the probability distribution is log-normal (see discussion by Sornette, 2006, pp 94–96). This last limitation is important since all hydrothermal systems and data sets have limited sizes. For a detailed discussion of power laws see Newman (2006).

4.1. Multifractal measures

The geometry of hydrothermal fabrics is more complicated than being characterised by a single value of D as we will see below. If the measure of an object is characterised by a single value of D then it is called a *monofractal*. Some measures are characterised by two values of D and these are called *bifractals*. However if the geometry is characterised by many different values of D at different points then the measure is clearly more complicated and is called a *multifractal* (Mandelbrot, 1974); a spectrum of D values arises; this spectrum is known as a *singularity spectrum*. A multifractal therefore consists of a set of interwoven fractal measures and is characterised by a spectrum of singularity measures. An example consists of a precipitation process, for say gold, that is itself fractal but is controlled spatially by a fractal distribution of the pore or fracture space within which precipitation occurs. The spatial distribution of gold concentration is then multifractal. For reviews of the development of the multifractal concept see Feder (1988); Bohr and Tel (1988); Beck and Schlogl (1993); Agterberg (1995); Arneodo et al. (1995), Schroeder (1991), and Sornette (2006). Discussions of the application of multifractals to sampling and to conventional

spatial statistics are in Cheng and Agterberg (1996) and Agterberg (2012).

Another way of thinking of irregular *measures* is in terms of homogeneity and heterogeneity. Fractal measures may be homogeneous in the sense that every part of the geometry is characterised by a single value of D in Eq. (3). Such geometry is called a *monofractal* geometry. However, most fractal measures are heterogeneous in the sense that different parts of the geometry are characterised by different values of D. These geometries are called *multifractal* geometries. Commonly in heterogeneous fractals, fractal sets with different values of D are intertwined at a fine scale (Fig. 7) and are difficult to analyse except by employing analytical techniques that can zoom into the fine scale. *Wavelet transforms* are one way of doing this.

In Fig. 7 the principles behind the development of a *multifractal* and its associated *singularity spectrum* are illustrated. In Fig. 7 (a) some of the attractors for the Kaplan-Yorke Map (Beck and Schlogl, 1993, p 11–12), given in Eq. (5), are plotted for the values of λ in Eq. (5) of 0.2, 0.3, 0.4 and 0.9; again they have been prepared using Excel. The Kaplan-Yorke map corresponds to a system where two chemical species compete for production.

$$\begin{aligned}x_{n+1} &= 1 - 2x_n^2 \\y_{n+1} &= \lambda y_n + x_n\end{aligned}\quad (5)$$

The attractors in Fig. 7 (a) are not differentiated so that points from each attractor are given the same colour. Fig. 7 (a) constitutes a set which is a fractal with fractal dimension, $D = 2$, the same as that of

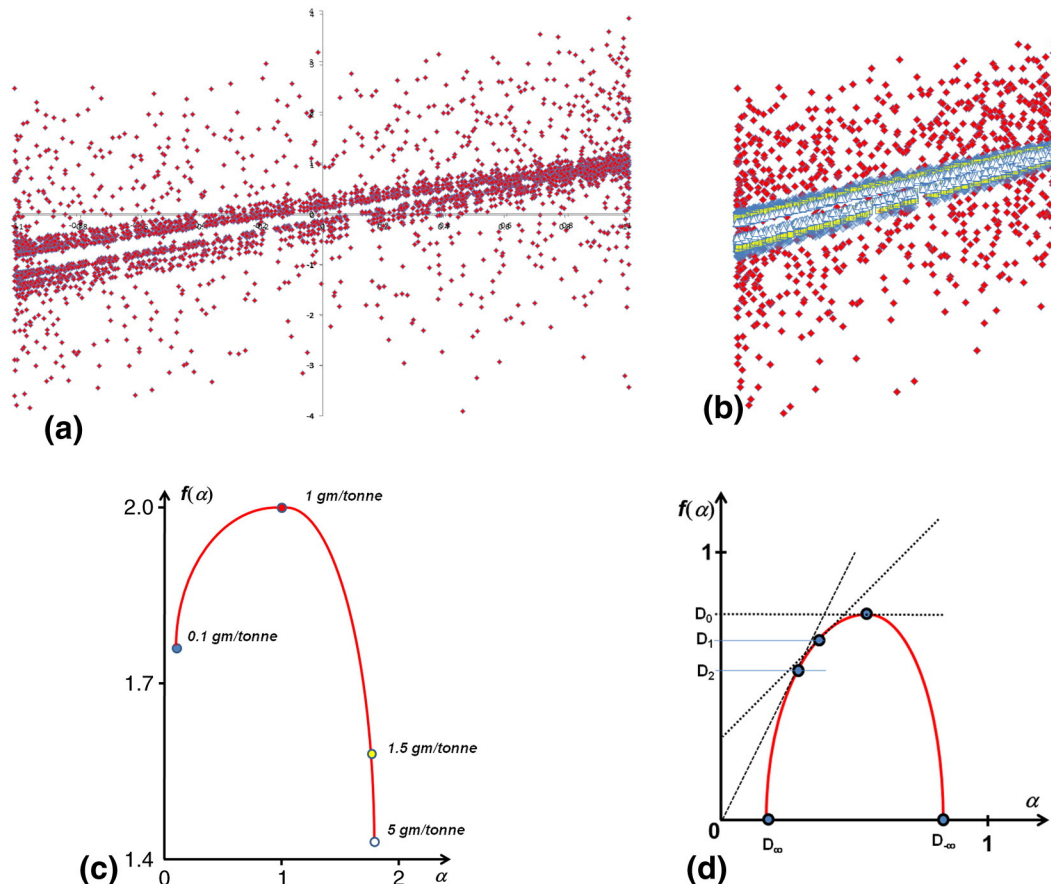


Fig. 7. A multifractal geometry. (a) This image consists of four monofractals, produced by the Kaplan-Yorke Map (Beck and Schlogl, 1993, p 11–12), embedded in each other. (b) Delineation of the four monofractals in (a) with $D = 1.43$ (white), $D = 1.58$ (yellow), $D = 1.76$ (blue) and $D = 2$ (red). These correspond to λ defined in (5) of 0.2, 0.3, 0.4 and 0.9 respectively. (c) Multifractal singularity spectrum arising from (b) where gold grades have been defined on the set described by (a) as a measure. (d) Singularity spectrum with commonly used metrics marked. D_0 , D_1 and D_2 are defined where the tangents with slopes of 0, 1 and 2 touch the singularity spectrum. D_∞ and $D_{-\infty}$ are the values of α where the singularity spectrum intersects the α -axis.

the sparsest attractor corresponding to $\lambda = 0.9$. In Fig. 7 (b) the four attractors in (a) are delineated by colour: white for $\lambda = 0.2$ ($D = 1.43$), yellow for $\lambda = 0.3$ ($D = 1.58$), blue for $\lambda = 0.4$ ($D = 1.76$) and red for $\lambda = 0.9$ ($D = 2.0$). These fractal dimensions are calculated from the discussion of the Kaplan-Yorke Map in Beck and Schlogl (1993, pp 268–270). We now associate, as an example, a gold grade with each colour: white: 5 ppm by weight; yellow: 1.5 ppm; red: 1 ppm and blue: 10^{-1} ppm. Fig. 7 (b) now constitutes a measure, which we call μ , representing the distribution of gold grade, superimposed on the fractal set defined by Fig. 7 (a). The set shown in Fig. 7 (a) is known as *the support for the measure*. We now define a quantity α , known as the *singularity strength*, by the relation (Chhabra and Jensen, 1989):

$$\alpha(q, \varepsilon) = \lim_{\varepsilon \rightarrow 0} \frac{\mu(q, \varepsilon) \ln P_\mu(\varepsilon)}{\ln \varepsilon} \quad (6)$$

and instead of proceeding to the limit we select a small value for ε of say 10^{-1} . α now takes on the values given in Table 1

Since $0 \leq P_\mu \leq 1$, and $\ln \varepsilon \rightarrow -\infty$ (a large negative number) as $\varepsilon \rightarrow 0$, α is always positive and is proportional to the gold concentration. $f(\alpha)$ is plotted against α in Fig. 7 (c). A \cap -shaped curve is produced which is typical of most multifractal distributions. The example illustrates that the low probability (high grade parts of the distribution) occupy the right hand limb of the singularity spectrum whereas the high probability (low grade parts) occupy the left limb.

One can see that the precise shape of the \cap -curve is quite sensitive to the ways in which the range of the measure and the ways in which the mono-fractals representing each value of the measure are distributed in space. If, for instance, all of the high gold grades are distributed over a wide range of fractal dimensions, from sparse to space filling, whilst the low grades have a restricted range of fractal dimensions, the \cap -shape is asymmetrical to the left and vice versa. Asymmetry in the singularity spectrum is an important feature (Drozd and Owsiecka, 2015) and indicates that different processes operate to produce the two sides of the spectrum. Left hand asymmetry indicates uniformity in the multiplicative processes responsible for the left hand side of the spectrum and more noise-like processes for the right hand side. If all low grades have much the same fractal dimension expressed as distributions that are space filling the singularity spectrum may be “one-sided” (Mandelbrot and Evertsz, 1991): \cap . If the highest and lowest grades are similar (the mineralisation is disseminated) then the arms of the \cap -shape are close together. If the highest and lowest grades are far apart (corresponding to a nuggety ore body) the \cap -shape is relatively open. Thus a measure of the asymmetry and width of the singularity spectrum are important metrics. The intersections of the singularity spectrum at its extremes on the left and right hand sides (Fig. 7d) are denoted as D_+ and D_- so that the quantity $(D_- - D_+)$ becomes an important quantity to compare different singularity spectra and in characterising mineralised systems. We will see in the Discussion that this metric is also a measure of criticality in a system and also of the presence or absence of long range interactions.

As a summary: A hydrothermal system is part of a lithospheric scale energy cascade whereby the deformation and fluid/heat flow within an element of the lithosphere is controlled at the largest of scales by the velocity boundary conditions imposed by the large scale tectonic regime

together with pressures (arising from the dead load exerted by the overlying rock mass and other contributions generated by topographic relief) and temperature changes arising from the impingement of heat sources and/or advection of the element through the geothermal gradient of the Earth. Such advection also contributes to changes in the pressure.

Thus at the coarse scale a deformation gradient drives momentum transfer whilst changes in temperature and pressure (both solid and fluid pressures) induce changes in chemical potentials that drive mineral reactions. In this process, forcing at lithospheric scales drives a cascade of dissipation at finer and finer scales within the lithosphere until at a very fine scale the dissipation is negligible. The development of lithospheric scale buckles and fault systems is part of a dynamical cascading process whereby structure is developed at finer and finer scales. At the coarse scale dissipation is dominated by deformation coupled with heat diffusion; at finer scales heat diffusion ceases to be dominant as a dissipative mechanism and the dissipative processes are dominated by local deformations, exothermal mineral metamorphic mineral reactions (alteration) and structural rearrangements such as fracturing, veining and brecciation. Finally energy is stored in endothermic mineral reactions (precipitation of sulphides, metals such as gold and anhydrous silicates such as feldspar). Such a cascading process is similar to that proposed for fluid turbulence where large eddies break down to shed eddies at smaller and smaller scales (Richardson, 1922; Drazin and Reid, 1981; Frisch, 1995; Kestener and Arneodo, 2003).

These cascading processes lead to multifractal geometries (Frisch, 1995, Chapter 8) and so it is of importance to develop efficient ways of measuring and characterising the scaling properties of structures in deformed, altered and mineralised rocks since there is the potential that such properties reflect the details of the cascading process. We use the *wavelet transform* method as a means of achieving this characterisation.

4.2. The wavelet transform

Although box counting procedures can be used to explore multifractal geometries, the process is quite cumbersome and can produce erroneous results especially if the singularity measure varies significantly within box sizes greater than a given value (see Arneodo et al., 1987, 1995). We require a fast, compact and quantitative characterisation of seemingly complex data sets that is readily applicable to 1, 2 and 3 dimensional situations and so we turn to a *wavelet* based system. The wavelet approach has many advantages over box counting procedures although a wavelet is basically a “generalised box”. Methods of multifractal analysis based on the wavelet transform are particularly applicable to self-similar, intermittent data sets where the wavelet acts as a “microscope” that can zoom into the details of the signal and define local structure and singularities. Wavelet based software now exists that makes fractal and multifractal analysis fast and efficient so that complex data sets can be completely analysed within minutes using a laptop computer. In addition the wavelet approach is reasonably well established within a thermodynamic framework (Bohr and Tel, 1988; Beck and Schlogl, 1993; Arneodo et al., 1995) so that the procedures and results can be placed within a broader mechanics framework.

The wavelet transform (WT) of a signal, s , consists of decomposing s into space-scale contributions that are defined by the *analysing wavelet*, ψ which is chosen to be localised in space and commonly of zero mean although $g^{(0)}$ (see Eq. (7)) is sometimes used where $g^{(0)}$ is the Gaussian function (Arneodo et al., 1995). A class of commonly used wavelets is defined by the successive derivatives of the Gaussian function given in Eq. (7) where N is the order of differentiation:

$$\psi(x) = g^{(N)}(x) = (-1)^{N+1} \frac{d^N}{dx^N} [\exp(-x^2/2)] \quad (7)$$

Table 1
Quantities used to construct the singularity spectrum, Fig. 7(c).

Gold grade, μ ppm by weight	Colour in Fig. 7(b)	Probability of occurrence, P_μ	$\alpha \approx \frac{\mu \ln P_\mu}{\ln(10^{-1})}$	$f(\alpha) \equiv D_{local}$
5	White	10^{-3}	1.765	1.43
1.5	Yellow	0.07	1.75	1.58
1	Red	0.1	1.0	2.00
0.1	Blue	0.1	0.1	1.76

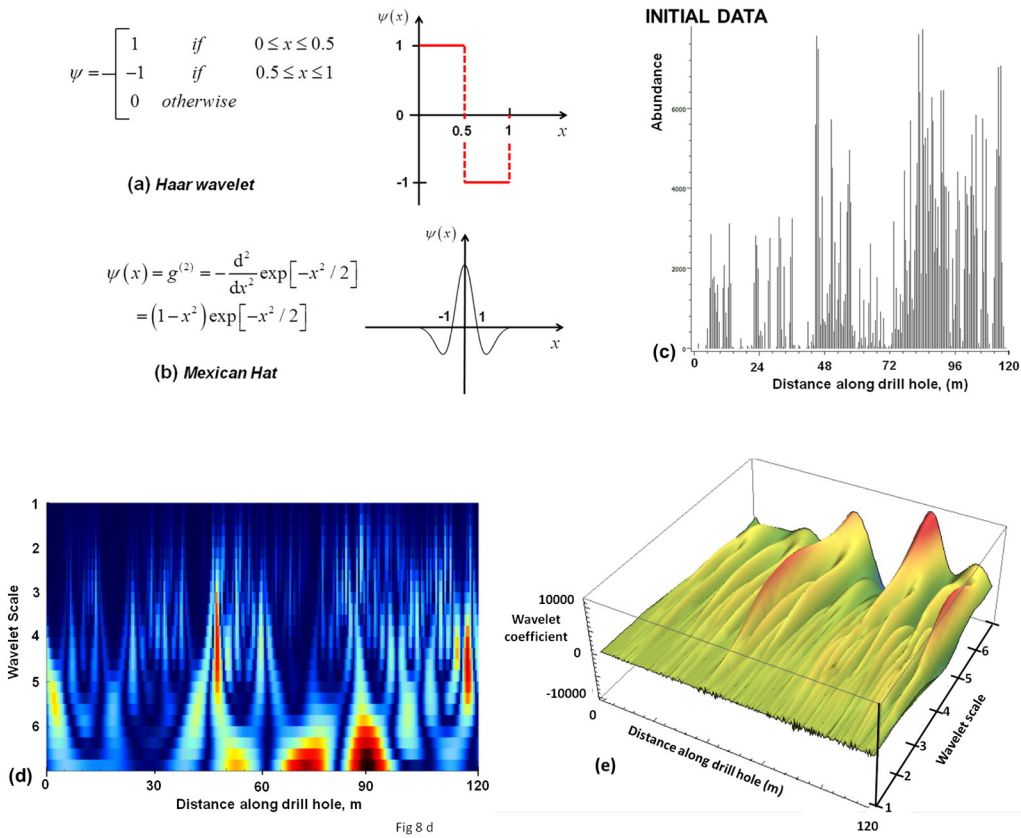


Fig. 8. The wavelet transform and scalogram. (a) The Haar mother wavelet which resembles a box in the classical box counting method. (b) The Mexican hat mother wavelet. (c) An example of a signal to be analysed. In this case a sequence of chlorite concentrations (see footnote 1) measured by infra-red reflectance along a 120 m long drill hole. (d) The wavelet transform of the signal in (c). This is also known as a scalogram. (e) A three dimensional version of the scalogram.

$g^{(2)}$ is shown in Fig. 8 (b). Note that various conventions are adopted in the literature with respect to the form of Eq. (7) and in some instances the $(-1)^{N+1}$ term is omitted. The WT of the function s is defined as the convolution of ψ with s :

$$W_\psi[s](b, a) = \frac{1}{a} \int_{-\infty}^{+\infty} \bar{\psi}\left(\frac{x-b}{a}\right) s(x) dx \quad (8)$$

where b is the space parameter (the place where the wavelet is centred), $a > 0$ is the scale parameter and $\bar{\psi}$ is the complex conjugate of ψ . The quantity $W_\psi[s](b, a)$ is known as the *wavelet coefficient* at the scale a , and around the point $x = b$. The procedure involved in a wavelet analysis is to select a *mother wavelet*, ψ , and contract or extend ψ by successive scales a . For each scale the wavelet is scanned across the image with the same procedure as for box counting so that $W_\psi[s](b, a)$ is evaluated at each point, b , and for each wavelet scale a . The local behaviour of s is reflected in the wavelet transform which behaves as

$$W_\psi[s](x_0, a) \sim a^{\alpha(x_0)} \quad (9)$$

where again, x_0 is a selected point and α is the *Hölder exponent*. Some examples of wavelet transforms are given in Figs. 8, and 10, through to Fig. 17. The wavelet transform contains all the information needed to establish the multifractal geometry of an object (Arneodo et al., 1995) and any correlations that might exist in the data set.

4.3. Correlations: the Hurst exponent

The wavelet transform gives information on the correlations between various parts of a signal such as that shown in Fig. 8 (c). We require knowing how parts of the signal correlate at different length

scales. In order to do this we use the Hurst exponent. Consider a one dimensional sequence of values, $\xi(d)$, representing the concentration of a particular mineral phase or the degree of fracturing or some other quantitative measure of the fabric of a hydrothermal system. In the example we take, ξ varies with distance, d , as shown in Fig. 9. We can characterise the resulting pattern in a number of ways. One way is to use the *Hurst exponent* (Feder, 1988; Sprott, 2003) which measures the way in which the local range in variation (or roughness) scales with distance

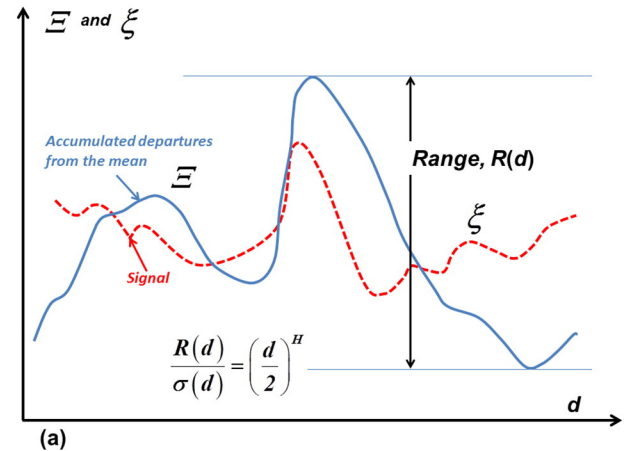


Fig. 9. Definition of the Hurst exponent, H . ξ is the initial data as a function of distance, d , and Ξ is derived from these data as the cumulative departure of the data from the mean. R is the range of Ξ , that is the difference between the maximum and minimum value of Ξ . If σ is the standard deviation of ξ , then the Hurst exponent is defined by $\frac{R}{\sigma} = (\frac{d}{2})^H$. Adopted from Feder (1988).

across the structure. In order to calculate the Hurst exponent we first take the mean of ξ and then (Fig. 9) the cumulative departures from the mean, $\Xi(d)$. If R is the range of Ξ , that is, the difference between the largest and smallest value of Ξ , then the Hurst exponent, H , is defined by:

$$\frac{R(d)}{\sigma(d)} = \left(\frac{d}{2}\right)^H \quad (10)$$

where $\sigma(d)$ is the standard deviation of ξ over the distance d . The characteristics of signals for various values of the Hurst exponent are given in Table 2. Hurst exponents and singularity spectra have been reported for a large number of styles of mineralisation by Liu et al. (2012) and Sun and Liu (2014).

4.4. Summary of work flow

The work flow involved in analysing a given data set is summarised below.

- The initial data set (Fig. 10a) is expressed in digital format. In some instances it may be useful to process the data in some manner to remove overall trends or to standardise the data interval. Details of these procedures are given in Sprott (2003).
- The wavelet transform is prepared as shown as a scalogram in Fig. 10 (b). This can be done using various software packages (Hobbs and Ord, 2015, p 236).
- The singularity spectrum is derived from the scalogram using suitable software. We have used *LastWave* (Arneodo et al., 2003) but other packages are available (see Hobbs and Ord, 2015, p 236). This singularity spectrum gives the metrics: D_0 , D_1 , D_2 , D_∞ and $D_{-\infty}$ (Fig. 10c).
- Profiles are prepared across the scalogram (Fig. 10b) as shown by the yellow lines. These can be at any convenient spacing. The profiles are shown in Fig. 10 (d).
- The Hurst exponent is calculated for each profile using Eq. (10). This can be done for the initial data set and for each of the profiles in Fig. 10 (d). The calculations can be readily done in Excel. The final results are plotted in Fig. 10 (e). In all scalograms and Hurst analyses the wavelet scale is given as octaves (see Appendix B).

In the results shown here the scalogram has been prepared using *Mathematica*; the singularity spectrum has been prepared using *LastWave*. The Hurst exponents have been calculated from the Mathematica derived scalogram.

5. Some examples from a gold deposit in the Yilgarn of Western Australia

As we have indicated, it is now routine to collect hyperspectral reflectance data for a large range of minerals such as chlorite, sericite and carbonates, including detailed changes in chemical composition,

in drill holes through hydrothermal systems. Also collected are multi-element chemical analyses and assays for gold. All this data is available in digital format and so is readily available for analysis using wavelet transforms. In what follows we give some examples of analyses from gold ore bodies in the Archean Yilgarn terrain of Western Australia. We select two deposits, namely the Sunrise Dam deposit (Hill et al., 2014) which is a large deposit comprised of a number of smaller rich deposits and Imperial (Munro et al., 2016) which is a small deposit with a small gold endowment. The example from Sunrise Dam is from the GQNorth part of the ore system (Hill et al., 2014). The aim is to provide examples of the results of processing these data sets. We also examine the multifractal nature of a breccia (Fig. 1d) from the Tropicana deposit (Blenkinsop and Doyle, 2014). Detailed results will be presented in a future paper. Even so, with the limited examples presented, important distinctions between the richly and poorly endowed deposits become clear.

In Figs. 11, 12 and 13 we present results for the GQNorth ore body within the Sunrise deposit in the Yilgarn of Western Australia (Hill et al., 2014). The Sunrise deposit is a high nugget deposit, currently owned by AngloGold Ashanti Australia and, at 30 June 2010, had resources of 23.3 million tonnes at 2.9 g/tonne Au for 2.17 million ounces of gold. The raw data for chlorite, sericite and gold for a drill hole 120 m long are presented in figure (a) of each of these figures whilst the scalogram is presented in (b), the singularity spectrum in (c) and the Hurst exponent at a number of scales in (d).

Figs. 14, 15 and 16 present similar data sets for chlorite, undifferentiated mica and gold, along a drill hole in the Imperial gold deposit (Munro et al., 2016) south of Kalgoorlie. In this example the drill hole is 100 m long. The Imperial deposit is presently owned by Silver Lake Resources and is small compared to Sunrise Dam with a resource quoted at 83,700 oz of gold.

As another example, Fig. 17 shows results for a breccia within a highly endowed gold deposit (Tropicana) in the Yilgarn of Western Australia. Fig. 17 (a) shows the breccia in a section of drill core. Fig. 17 (b) shows the singularity spectrum for a one dimensional section along the centre of the core. Fig. 17 (c) is the singularity spectrum and (d) shows the Hurst exponents at various scales on the scalogram.

6. Discussion

The Yilgarn mineralised systems illustrated in this paper show the following three characteristics:

- (i) All data sets, whether they be for gold, chlorite, sericite (or mica) or breccia show well developed singularity spectra that differ quite strongly from those obtained for monofractal signals and white noise (Ihlen, 2012). This shows that although the signals appear to be stochastic they have an underlying deterministic origin. This is encouraging because it carries the promise that with further analysis (Arneodo et al., 1995) we can learn more about the underlying physical and chemical processes involved in the formation of these systems. Ideally we would like to establish the attractor for these systems since that would give clues regarding the details of the underlying mathematical framework. The construction of an attractor however requires more data than we have been able to assemble so far. The various spectra show a range of values for the metrics, D_0 , D_1 and D_2 (Fig. 10c) which we will not explore any further here. Instead we concentrate on the values of $(D_{-\infty} - D_{+\infty})$.
- (ii) The values of $(D_{-\infty} - D_{+\infty})$ for various spectra are summarised in Fig. 18 (a). They clearly fall into two groups; the well-endowed deposit (Sunrise Dam) shows a very large value of $(D_{-\infty} - D_{+\infty})$ for gold relative to the less endowed deposit (Imperial). The chlorite and sericite values of $(D_{-\infty} - D_{+\infty})$ are close together for Sunrise Dam and well separated for Imperial. Of course the data set is very small and we will report on larger data sets in

Table 2
Characteristics of the Hurst exponent, H , for a one dimensional signal.

Value of H	Meaning	Pattern characteristics
$0.5 < H < 1$ Persistent	Long range positive autocorrelations	A high (low) value tends to be followed by another high (low) value. The overall trend is to higher (lower) values. Power law decay in autocorrelations.
$H = 0.5$	Completely uncorrelated sequence.	Autocorrelations at small intervals can be positive or negative. Absolute value of autocorrelations decays rapidly to zero.
$0 < H < 0.5$ Antipersistent	Long range switching between high and low values	A high value tends to be followed by a low value. Power law decay in autocorrelations.

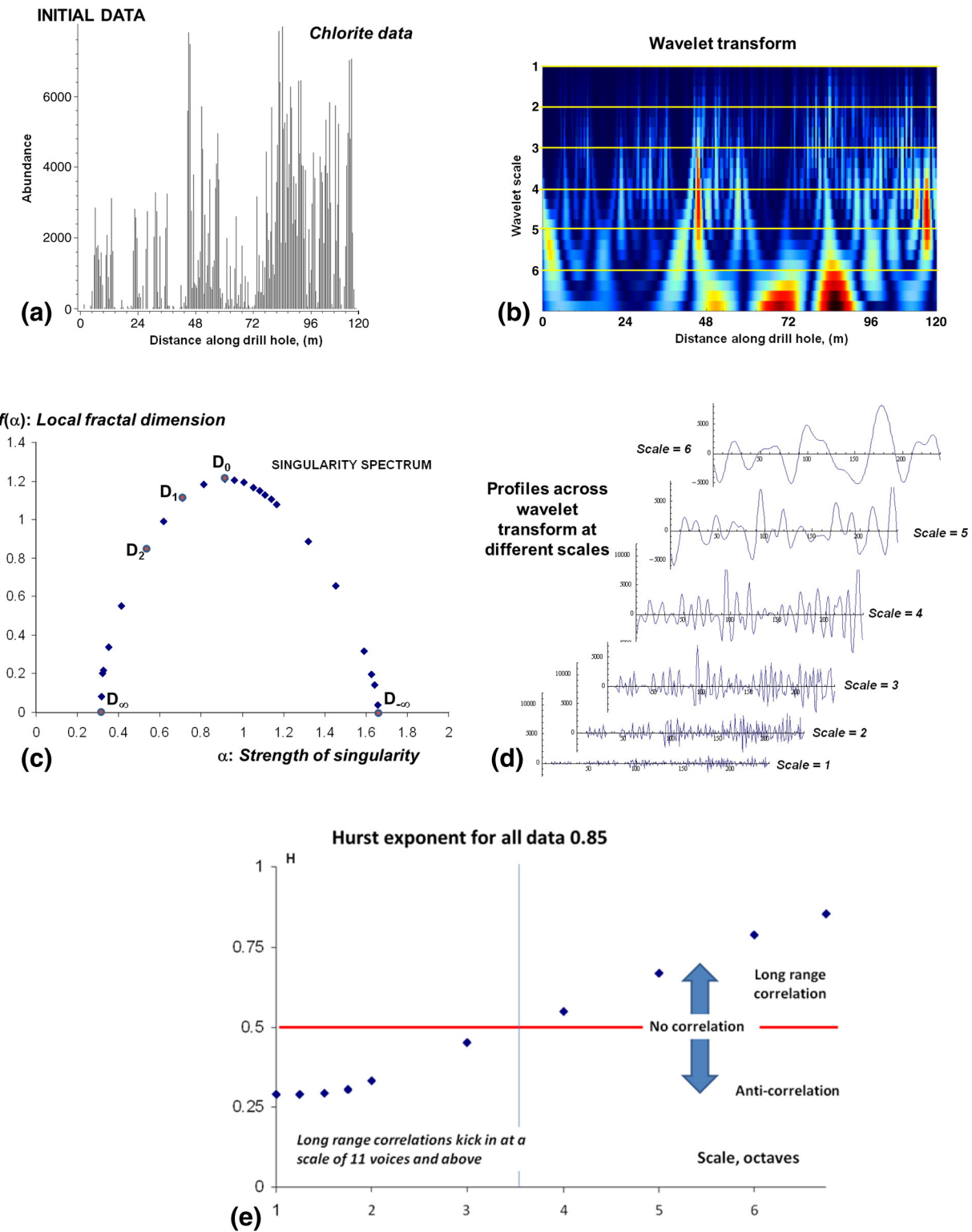


Fig. 10. Summary of work flow in analysing data. (a) The raw data. Chlorite hyperspectral data collected at 0.5 m intervals along a diamond drill core (see footnote 1). (b) Wavelet transform scalogram of the data. Yellow lines indicate the section profiles shown in (d). (c) Singularity spectrum with important indices, D_0 , D_1 , D_2 , D_∞ , and $D_{-\infty}$, labelled. (d) Sections across the scalogram in (b). (e) Hurst exponents for each section line in (b). Hurst exponent for the raw data is 0.85. Long range correlations begin at 11 voices which corresponds to ≈ 0.9 m marked by the vertical blue line. At less than 8 voices, it is an artefact of the process that the wavelet scale is smaller than the sampling scale.

Munro et al. (2016). As an indication of results from larger data sets we show in Fig. 18 (b) results from Cosmo East (a part of Sunrise Dam) and Salt Creek (with a resource of 109,390 oz of gold). Again the high resource deposit (Cosmo East) shows a large proportion of values for $(D_{-\infty} - D_{+\infty})$ in the range 4 to 8 whereas the smaller resource deposit (Salt Creek) has a peak at

$(D_{-\infty} - D_{+\infty}) \approx 2$. Cosmo East also has this peak suggesting that the deposit has some less endowed parts. Both deposits have similar values of $(D_{-\infty} - D_{+\infty})$ for chlorite. In Fig. 19 we show a model proposed by Zapperi et al. (1995) and discussed by Ihlen and Vereijken (2010). The model is a cellular automata that activates adjacent nodes according to a

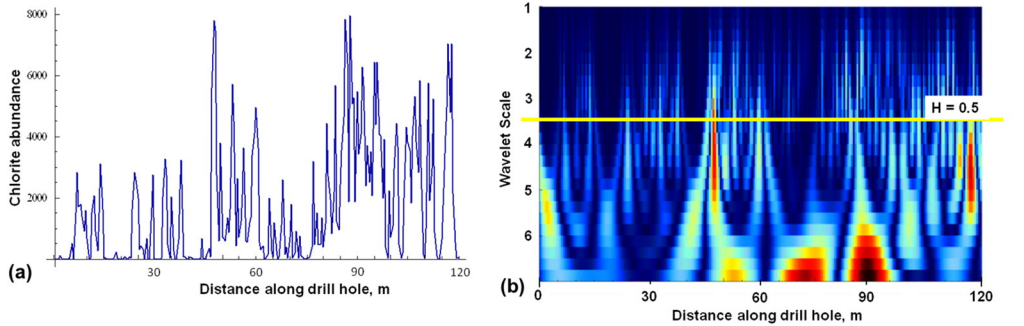


Fig. 11. Scalograms and Hurst exponents for chlorite data, Sunrise Dam (GQNorth), Western Australia. Drill hole length 120 m, sampled at 0.5 m intervals. (a) Near infra-red reflectance data (see footnote 1). (b) Scalogram. The yellow line indicates where the Hurst exponent changes from <0.5 to >0.5. (c) Singularity spectrum. ($D_{-\infty} - D_{+\infty}$) ≈ 1.35 (d) Hurst exponents at various scales showing where the Hurst exponent changes from <0.5 to >0.5. The cross-over scale is quoted as a voice (see Appendix B). In this case 11 voices corresponds to ≈ 0.9 m.

probability, p . If $p < 0.5$ the model evolves to a sub-critical state with relatively small values of $(D_{-\infty} - D_{+\infty})$. At $p = 0.5$, which corresponds to a critical state, $(D_{-\infty} - D_{+\infty})$ suddenly increases

and attains relatively high values for $p > 0.5$, corresponding to supercritical states. This model is a form of self-organised criticality. Very similar results are obtained by Ihlen and Vereijken (2010)

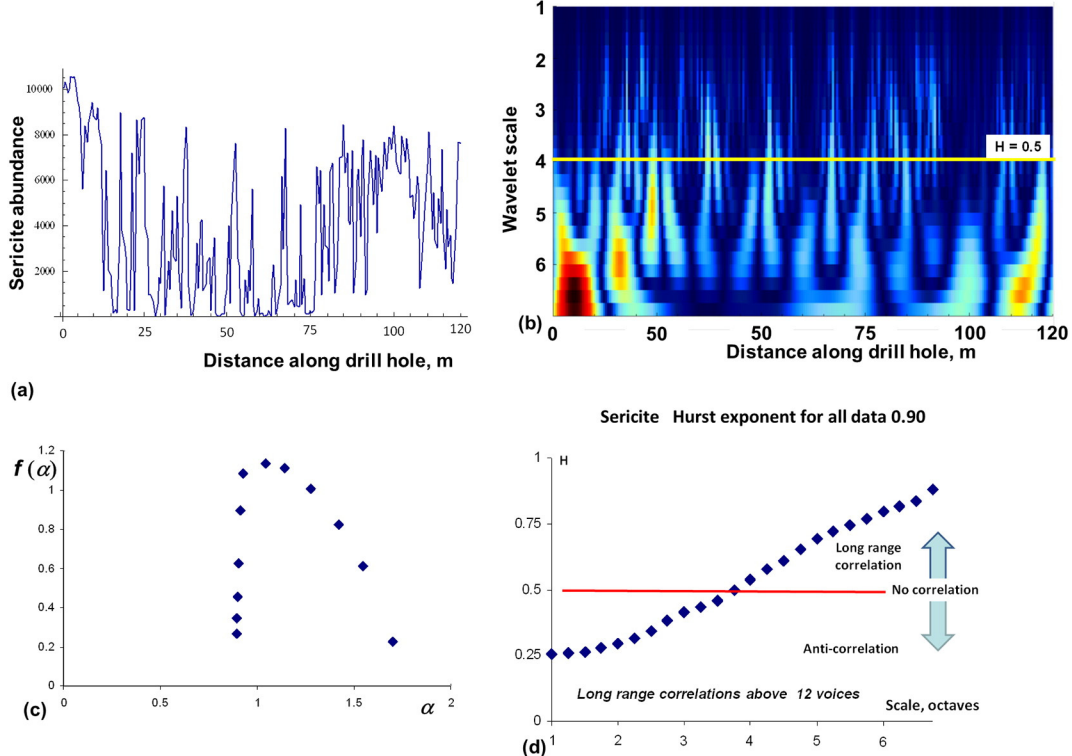


Fig. 12. Scalograms and Hurst exponents for sericite data, Sunrise Dam (GQNorth), Western Australia. (a) Near infra-red reflectance data (see footnote 1). Data collected at 0.5 m intervals. (b) Scalogram. The yellow line indicates where the Hurst exponent changes from <0.5 to >0.5. (c) Singularity spectrum. ($D_{-\infty} - D_{+\infty}$) ≈ 1 (d) Hurst exponents at various scales showing where the Hurst exponent changes from <0.5 to >0.5. The cross-over scale is quoted as a voice (see Appendix B). In this case 12 voices corresponds to ≈ 1 m.

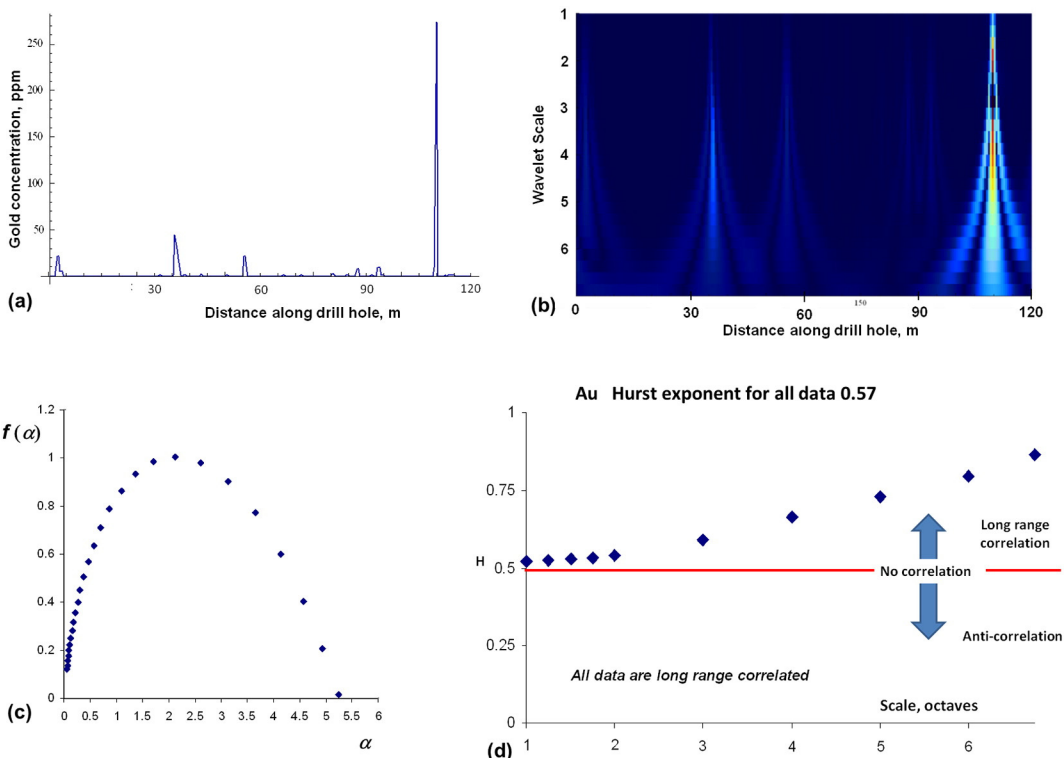


Fig. 13. Scalograms and Hurst exponents for gold data, Sunrise Dam (GQNorth), Western Australia. Drill hole length 120 m, sampled at 0.5 m intervals. (a) Assay data. (b) Scalogram. The yellow line indicates where the Hurst exponent changes from <0.5 to >0.5. (c) Singularity spectrum. ($D_{-\infty} - D_{+\infty}$) ≈ 5.25 . (d) Hurst exponents at various scales showing that the Hurst exponent changes from near to 0.5 at small spatial scales to >0.5 at larger scales.

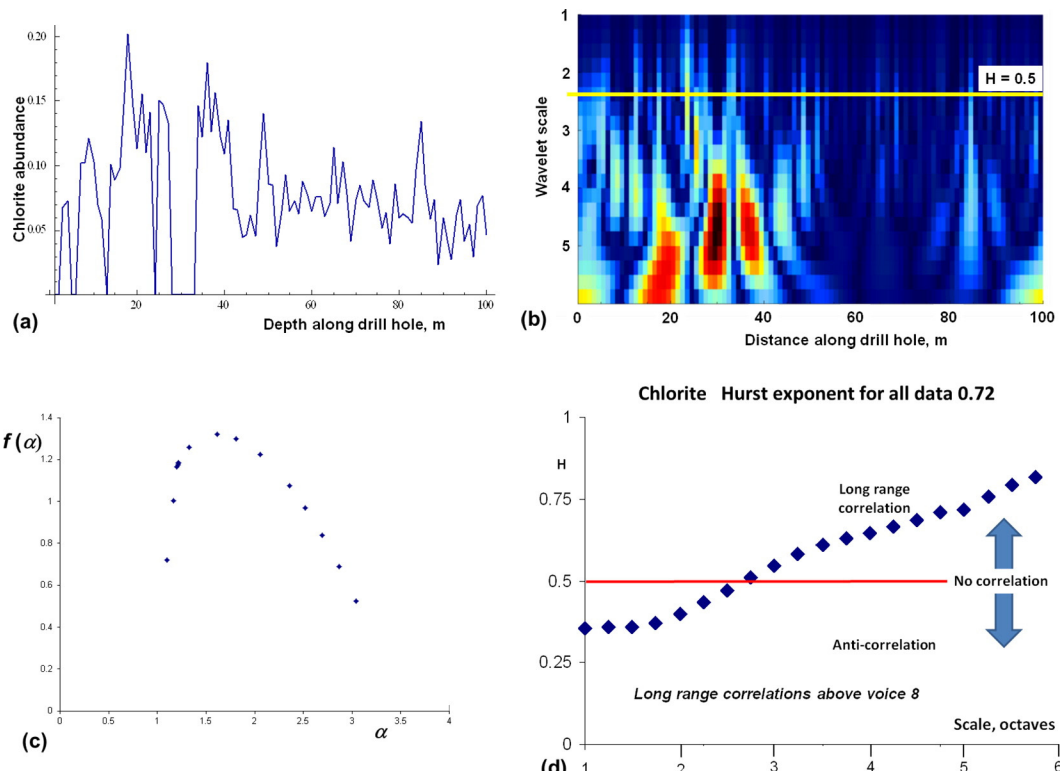


Fig. 14. Multifractal geometry of chlorite abundance (see footnote 1) from Imperial mine, Yilgarn, Western Australia. Drill hole length 100 m, sampled at 1 m intervals. (a) Abundance hyperspectral data. (b) Scalogram for data in (a). (c) Singularity spectrum for data in (a). ($D_{-\infty} - D_{+\infty}$) ≈ 2.5 (d) Hurst exponents for scalogram in (b). The cross over scale of 8 voices from uncorrelated to correlated corresponds to ≈ 1 m.

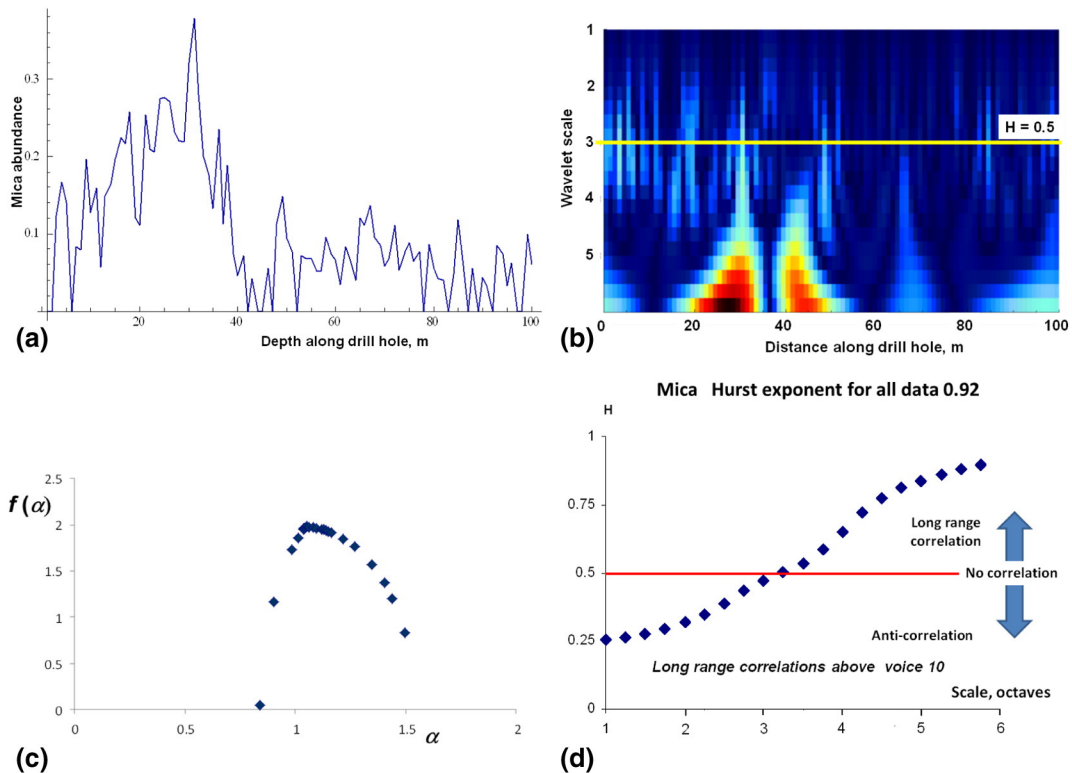


Fig. 15. Multifractal geometry of mica abundance (see footnote 1) from Imperial mine, Yilgarn, Western Australia. Drill hole length 100m, sampled at 1 m intervals. (a) Abundance hyperspectral data. (b) Scalogram for data in (a). (c) Singularity spectrum for data in (a). (d) Hurst exponents for scalogram in (b). The cross over scale of 10 voices from uncorrelated to correlated corresponds to ≈ 1.4 m.

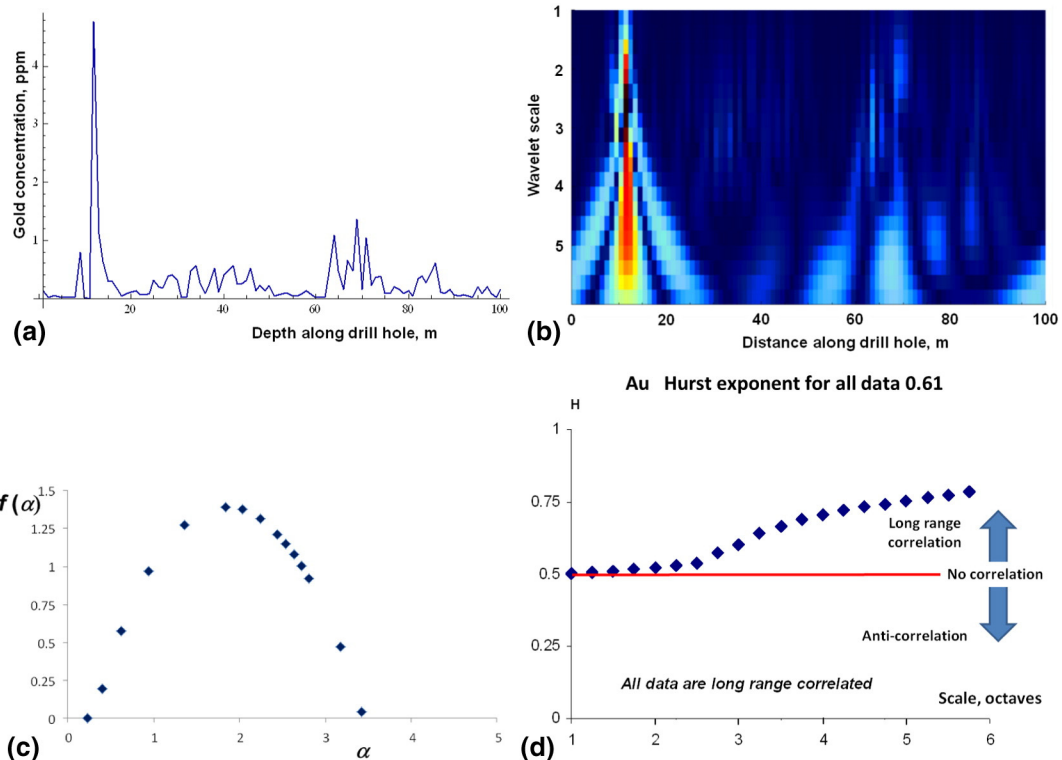


Fig. 16. Multifractal geometry of gold concentration from Imperial mine, Yilgarn, Western Australia. Drill hole length 100 m, sampled at 1 m intervals. (a) Assay data each 1 m along hole. (b) Scalogram for data in (a). (c) Singularity spectrum for data in (a). ($D_{-\infty} - D_{+\infty} \approx 3.1$) (d) Hurst exponents for scalogram in (b) showing that the Hurst exponent is near to 0.5 at small spatial scales and increases to >0.5 at coarser scales.

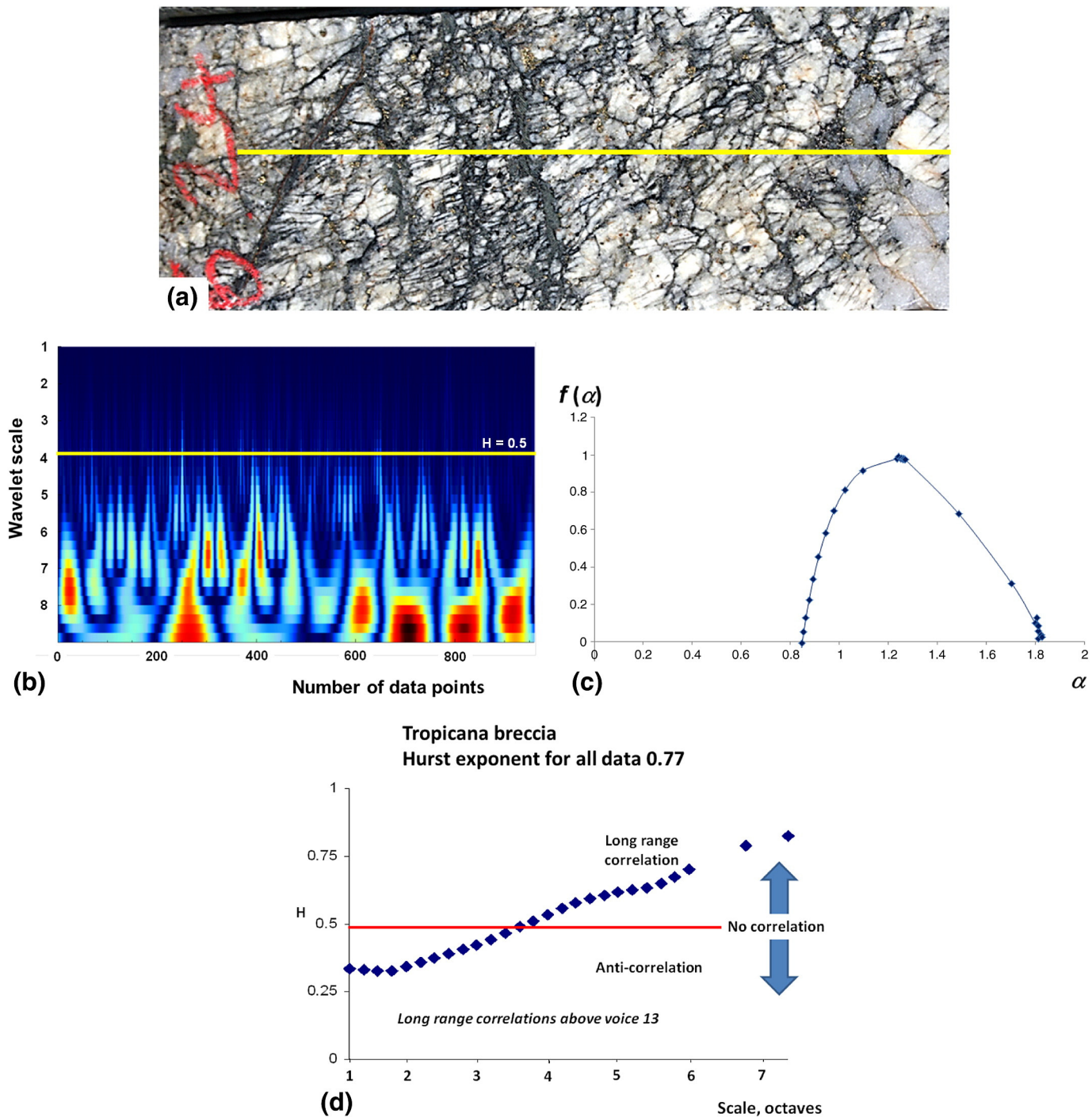


Fig. 17. Highly mineralised breccia from the Tropicana deposit, Western Australia. (a) Drill core showing the breccia. Profile line shown in yellow. Image is 12 cm long. (b) Wavelet transform of section across (a). (c) Singularity spectrum derived from (b). ($D_{-\infty} - D_{+\infty} \approx 1$) (d) Hurst exponents at various spatial scales. Voice 13 corresponds to ≈ 0.24 mm.

for a multiplicative cascade process due to Chainais (2006); this model does not propose self-organised criticality as an inherent process. If one adopts the Ihlen-Vereijken model, the data reported here suggest that well-endowed ore bodies are super-critical whereas less endowed ore bodies are sub-critical and this is reflected in $(D_{-\infty} - D_{+\infty})$ values.

- (iii) All data sets show short range (≤ 1 m) anticorrelation behaviour ($H < 0.5$) or no spatial correlations ($H = 0.5$). Above this cross-over spatial scale and up to the longest scales sampled (800 m) long range positive correlations develop. This suggests that two

different processes operate in this system, one at length scales less than about 2 m and the other at longer length scales.

We present in Fig. 20 the results of a coupled mechanical-fluid flow model that demonstrates this same behaviour. The material modelled is in the form of a rectangle, 1000 m long and 100 m wide with porous Mohr-Coulomb constitutive behaviour. The constitutive properties are given in Table 3. The model is fully saturated and is shortened vertically as shown in Fig. 20 (a) with fluid flow driven by an imposed fluid

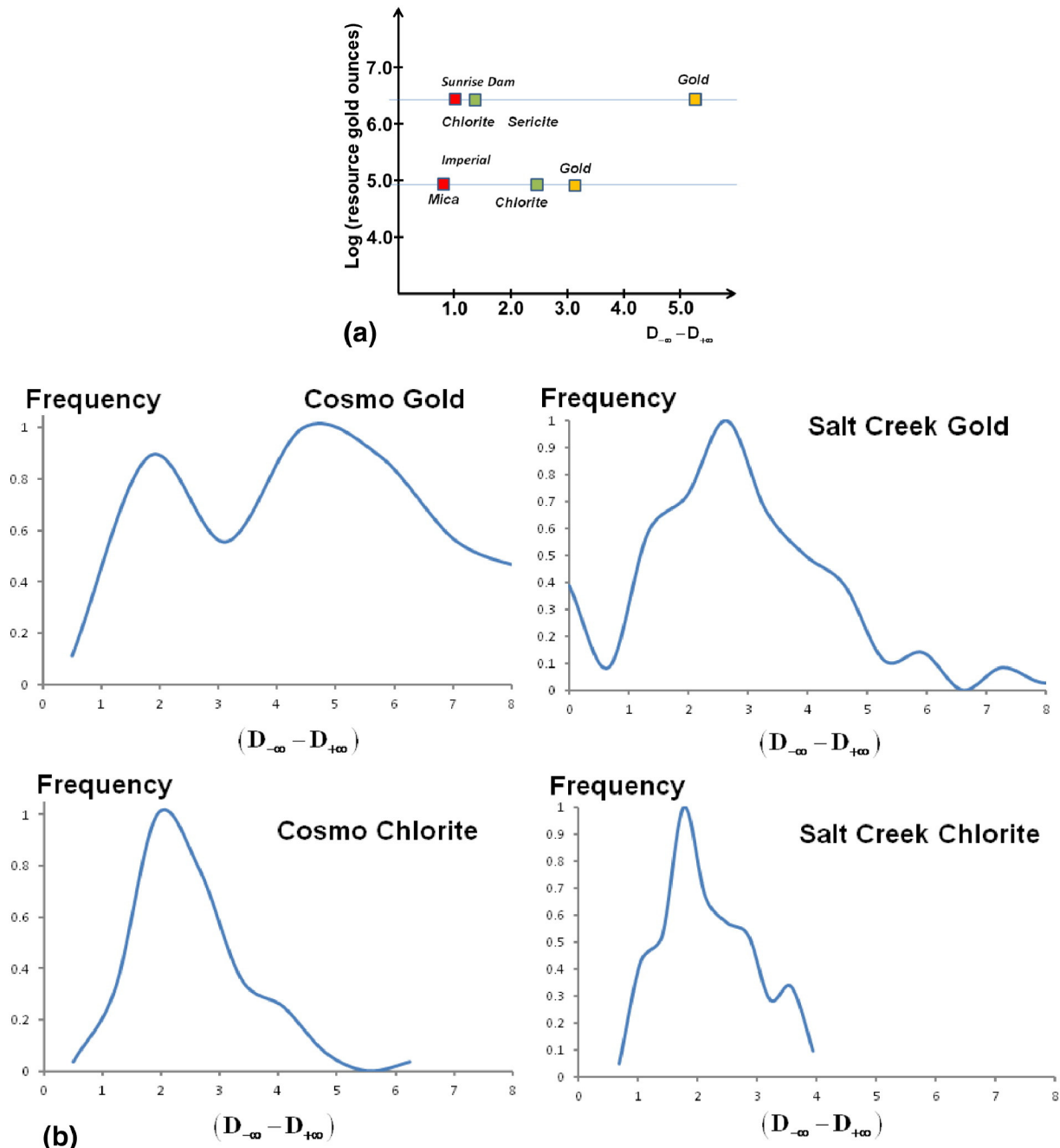


Fig. 18. Synthesis of $(D_{-\infty} - D_{+\infty})$ data. (a) $(D_{-\infty} - D_{+\infty})$ data from GQNorth and Imperial ore bodies, Sunrise Dam. (b) Normalised frequency $(D_{-\infty} - D_{+\infty})$ data from Cosmo East (Sunrise Dam) and Salt Creek ore bodies. Numbers of samples: 40 gold, Cosmo East. 79 chlorite, Cosmo East. 170 gold, Salt Creek. 93 chlorite, Salt Creek.

pressure gradient from left to right. The material fails in the form of conjugate shear zones (Fig. 20b) which focus fluid flow as shown in Fig. 20 (c) on the scale of 10 m or so. Long range correlated flow is shown in Fig. 20 (d). Although shear zones develop in this model no change in permeability is incorporated as a result of shearing. The permeability remains constant at 10^{-16} m^2 . Focussing of fluid flow arises from the fluid pressure drop in the dilatant shear zones. The otherwise uniform flow from left to right is modified to form a somewhat irregular pattern governed by local plastic dilatancy in the shear zones.

Fig. 20 (e) presents data on the Hurst exponent for fluid pressure at different scales within the model. There is a cross-over from anti-correlated to strongly correlated at approximately 7 m.

This means that fluid is focussed into the shear zones in the form of cells approximately 5 to 10 m across and a strong component of non-longitudinal flow is added at this scale to the overall longitudinal flow.

We propose that this non-longitudinal flow enhances fluid mixing and increases the overall yield of the reactor-system. Such enhancement of yield by non-longitudinal flow is well documented in experimental and commercial chemical reactors (Weinstein and Adler, 1967; Felder and Hill, 1969; Villermaux, 1986; Ottino, 1994; Baldyga and Pohorecki, 1995; Tang and Boozer, 1999). We speculate, following experience in experimental and commercial reactors, that without this window of anti-correlation or of no correlation within the system low yields of mineralisation would result.

Thus although the Constructal Law (Section 1) of Bejan and Lorente (2008) is an important expression of the flow system that needs to be established in a well mineralised system another important ingredient is expressed by rewriting this law as: *for a finite-size flow system to persist in time (to live) it must evolve such that it provides greater and greater access to the currents that flow through it. For the system to be strongly*

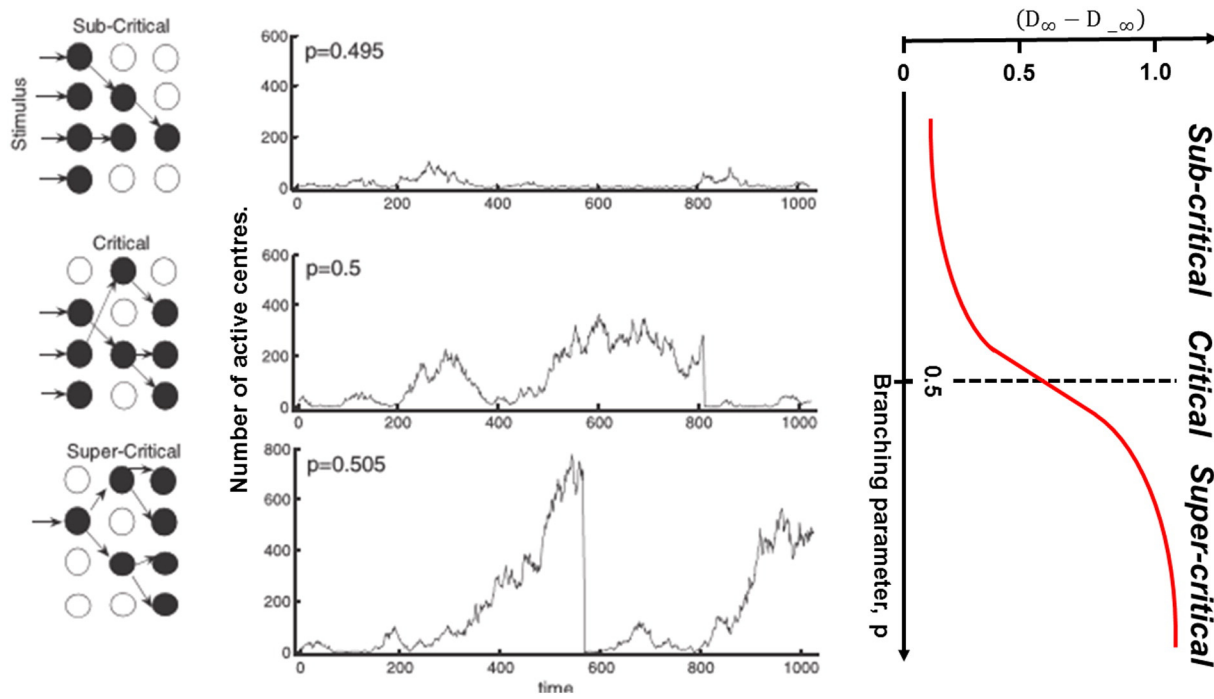


Fig. 19. Results of self-organized branching process (after Ihlen and Vereijken, 2010). Left column portrays the model whereby an initial array of centres (black: active and white: inactive) gives rise to other centres with a probability of formation, p . If $p < 0.5$ the likelihood is that inactive centres will be produced and the process ultimately stops. The resultant signal is given in the top central panel. If $p = 0.5$ the behaviour is given in the centre panel (middle). If $p > 0.5$ strongly intermittent behaviour results as in the centre panel, bottom. The behaviour of the quantity $(D_{-\infty} - D_{+\infty})$ as p varies from 0 to 1 is given in the right panel. $(D_{-\infty} - D_{+\infty})$ varies from small values for $p < 0.5$ to larger values for $p > 0.5$.

mineralised these currents must also undergo chaotic mixing arising from sub-cells within the flow currents.

7. Conclusion

In viewing hydrothermal mineralising systems as open flow chemical reactors it becomes clear that these systems, in order to continue operating, undergo a number of phase changes. The dominant transitions are unaltered \rightarrow altered, which is an exothermic transition, un-mineralised \rightarrow mineralised, which is an endothermic transition, and undeformed \rightarrow veined/brecciated, which is a combination of exothermic (fracturing, breakage, precipitation of carbonates and quartz) and endothermic (precipitation of sulphides and non-hydrous silicates such as albite) processes. The competition between these processes means that the reactor behaves in a non-linear, chaotic manner with chaotic spatial distributions of alteration, mineralisation and veining/brecciation.

Although chaotic, all of these spatial distributions are deterministic in origin even though they appear as apparently stochastic patterns. Such patterns are multifractal and the deterministic origin is revealed in singularity spectra that are significantly broader than spectra arising from white noise. The width, $(D_{-\infty} - D_{+\infty})$, of these spectra appear to be related to the mineralised endowment of the system so that weakly endowed systems have narrow spectra whereas strongly endowed systems have wide spectra. This can be interpreted as a transition from sub-critical to super-critical behaviour if one adopts a self-organised critical model or as a transition from weak to strong long range interactions if one adopts a multiple-cascade model.

All systems show long range spatial correlations if one uses the raw data but if one measures the spatial correlations at individual length scales, these systems show short range anti-correlations and long range positive correlations. We propose that the short range anti-correlations correspond to relatively small fluid mixing cells of the order of 10 m across that are responsible for the intensity of mineralisation and alteration. The long range spatial correlations indicate that the system has established a correlated fluid flow system on

the scale of the sampling length. It is notable that at small spatial scales gold distribution has Hurst exponent close to 0.5 which means that at that scale gold distributions are uncorrelated. Any correlations arise at relatively large spatial scales.

Acknowledgements

This project is funded by grants from the Australian Research Council (Project: LP100200785, Multiscale Dynamics of Ore Body Formation), and MRIWA (Project: M424, Multiscale Dynamics of Hydrothermal Mineral Systems). We thank The Geological Survey of Western Australia, First Quantum Minerals Ltd., AngloGold Ashanti, and Silver Lake Resources for financial support and access to data. We also thank Greg Hall, Julian Vearncombe and Marcus Willson for encouraging us to explore non-linear systems. Sarah Firth, Sandi Occhipinti, Tony Roache, Catherine Spaggiari and Ian Tyler are thanked for discussions and facilitating access to data.

Appendix A. The mathematical equations that describe the operation of a mineralising reactor

As we saw in the [Introduction](#) the equations governing the behaviour of a reactor are of the form

- Mass balance.
- Heat transfer.
- Fluid transport including the coupled mechanics of permeability generation and destruction.
- Chemical reaction kinetics including the *chemical* mechanisms of permeability generation and destruction.
- Mechanical deformation including the *mechanical* mechanisms of permeability generation and destruction.

There are many examples of equations that have been written to describe the behaviour of chemical reactions including [Aris \(1961, 1978\)](#);

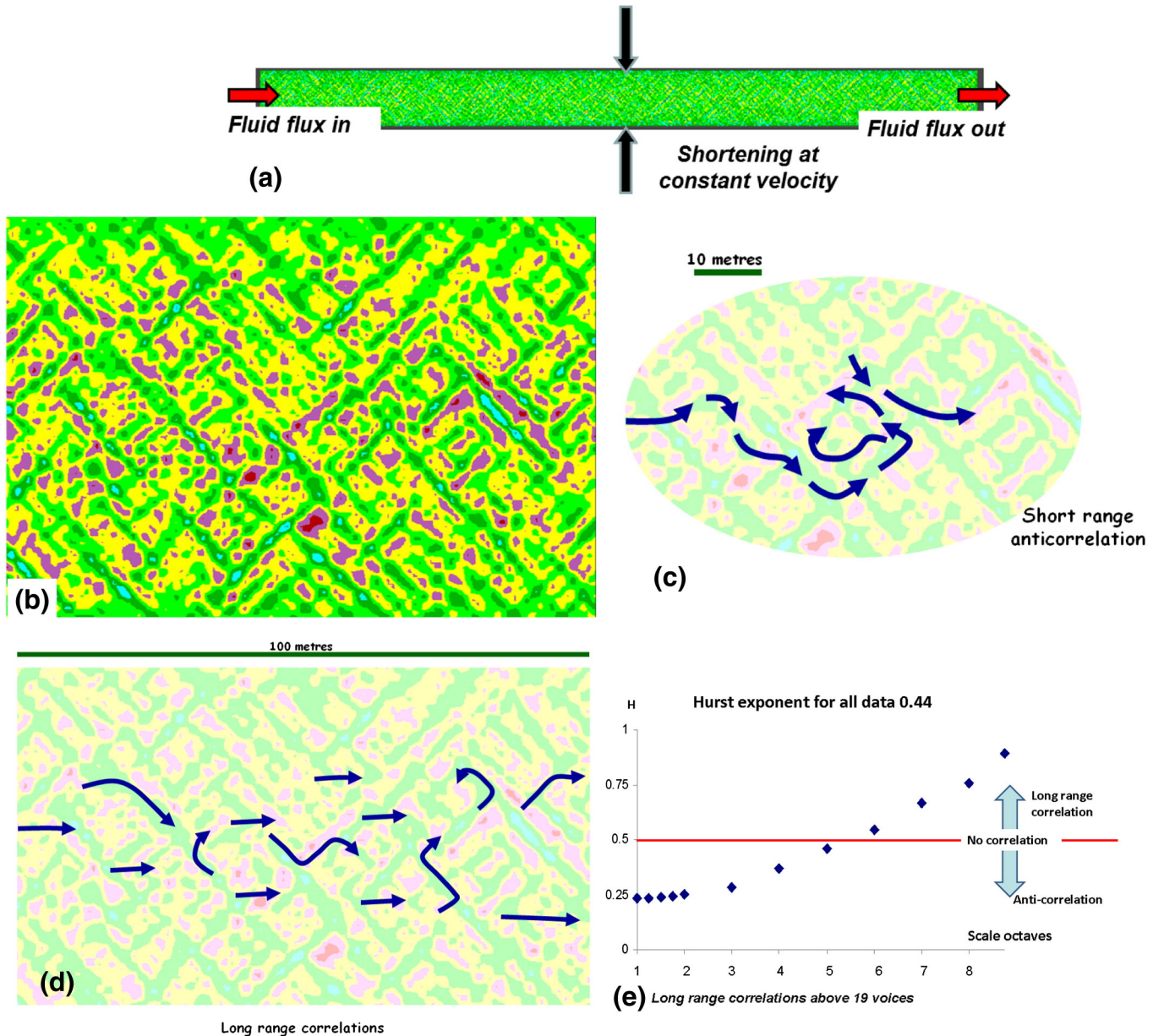


Fig. 20. Computational model of fluid flow in a deforming Mohr-Coulomb material. The material localises into shear zones that control fluid flow. (a) The model set up. (b) Shear localisation marked by contours of instantaneous strain rate. Zones of localisation correspond to zones of high plastic dilatancy. (c) Sketch of fluid flow vectors at the scale of 10 m. (d) Sketch of fluid flow vectors at a scale of 100 m. (e) Hurst exponents at various scales derived from a scalogram of the instantaneous strain rate pattern in figure (b). The cross over scale of 19 voices corresponds to ≈ 7 m.

Lynch et al. (1982); Gray and Scott (1994); Epstein and Pojman (1998) and Berozowski (2014) (and references therein). We consider a very simple reactor where two reactants, A and B, form products C and D according to $A \xrightarrow{E_1} k_1 C$ and $B \xrightarrow{E_2} k_2 D$ where k_1 , k_2 and E_1 , E_2 are the reaction constants and activation energies of the two reactions. Both reactions are assumed to be exothermic and follow first order Arrhenius rate

laws. The mass balance relations are of the form

$$\left[\begin{array}{l} \text{Rate of change of} \\ \text{number of moles of} \\ A \text{ in the reactor} \end{array} \right] = \left[\begin{array}{l} \text{Rate of addition} \\ \text{of } A \text{ to the} \\ \text{reactor} \end{array} \right] - \left[\begin{array}{l} \text{Rate of removal} \\ \text{of } A \text{ from the} \\ \text{reactor} \end{array} \right] + \left[\begin{array}{l} \text{Rate of production} \\ \text{of } A \text{ in the reactor} \end{array} \right].$$

For these reactions Lynch et al. (1982) write the mass balance relations in the form

$$V \frac{d[A]}{dt} = Q([A_0] - [A]) - V[A]k_1 \exp\left(-\frac{E_1}{RT}\right) \quad (\text{A1})$$

$$V \frac{d[B]}{dt} = Q([B_0] - [B]) - V[B]k_2 \exp\left(-\frac{E_2}{RT}\right) \quad (\text{A2})$$

Table 3

Constitutive parameters for model in Fig. 20.

Constitutive parameter	Value
Bulk modulus	1.0 GPa
Shear modulus	1.0 GPa
Cohesion	10 MPa
Friction angle	30°
Dilation angle	2°
Permeability	10^{-16} m^2

where V is the volume of the reactor, R is the gas constant, Q is the volumetric entrance flow rate and $[A_0]$, $[A]$ and $[B_0]$, $[B]$ are the feed concentrations and local concentrations of A and B. t is time. The energy balance of the reactor is expressed as

$$\begin{bmatrix} \text{Rate of change} \\ \text{of energy of} \\ \text{the reactor} \end{bmatrix} = \begin{bmatrix} \text{Rate of energy} \\ \text{released by} \\ \text{reactions} \end{bmatrix} - \begin{bmatrix} \text{Rate of energy} \\ \text{added in the} \\ \text{flow} \end{bmatrix} \\ + \begin{bmatrix} \text{Rate of energy} \\ \text{extraction in} \\ \text{the flow} \end{bmatrix} - \begin{bmatrix} \text{Rate of energy} \\ \text{removed by} \\ \text{heat transfer} \end{bmatrix}$$

which Lynch et al. (1982) write as

$$V\rho c_p \frac{dT}{dt} = H_{r_1} V[A]k_1 \exp\left(-\frac{E_1}{RT}\right) + H_{r_2} V[B]k_2 \exp\left(-\frac{E_2}{RT}\right) - Q\rho c_p(T-T_0) - SU(T-T_0) \quad (\text{A3})$$

where T_0 , T are the feed and reactor temperatures, ρ is the density, c_p is the isobaric specific heat, H_{r_1} , H_{r_2} are the heats of reaction for reactions 1 and 2, S is the surface area of the reactor where heat is lost and U is the reactor heat transfer coefficient.

Lynch et al. (1982) show that the system of equations (A1), (A2) and (A3) display a range of oscillatory behaviours depending on the ratios $\beta = \frac{H_{r_1}}{H_{r_2}}$ and the Damköhler Number, $\frac{V}{Q} k_1 \exp\left(-\frac{E_1}{RT}\right)$. Moreover, since there are three differential equations involved, the system can show chaotic behaviour depending on both β and the ratio, $\frac{E_1}{E_2}$. The attractors derived from these equations resemble classical attractors discussed by Sprott (2003) and Beck and Schlögl (1993) where multifractal geometries are documented.

The reactor described by Eqs. (A1), (A2) and (A3) is the simplest reactor one can consider where the reactions are coupled only by temperature. More complicated versions where the reactions are coupled by mass transfer and the reactions are autocatalytic are considered by Gray and Scott (1994). Coupled exothermic/endothermic reactions are considered by Kahlert et al. (1981). If reaction-diffusion reactions are included (Epstein and Pojman, 1998), spatio-temporal chaos arises. Several examples of chaotic behaviour in coupled reactors are considered by Berozowski (2014) (and references therein). Deformation is not included in any of the classical treatments of chemical reactors. Deformation is responsible for evolution of permeability and this adds yet another set of equations ensuring that chaos is an essential ingredient in the evolution of the reactor.

Appendix B. The scalogram and wavelet transform

In Mathematica® a scaling parameter, s , of the wavelet signal is defined in terms of an equal tempered scale given in powers of 2 and divided into octaves and subdivided into 4 “voices”. Thus the scaling parameter is divided into the array expressed in Eq. (B.1).

$$\begin{aligned} [1, 1, 1, 2, 1, 3, 1, 4] & \quad \text{octave 1, voices 1 to 4.} \\ [2, 1, 2, 2, 2, 3, 2, 4] & \quad \text{octave 2, voices 5 to 8} \\ \dots & \quad \text{octave } n_{oct}, \text{ voices}(4 n_{oct} - 3) \text{ to } 4 n_{oct} \end{aligned} \quad (\text{B.1})$$

n_{oct} is the total number of octaves representing the wavelet signal and is given by

$$n_{oct} = \left\lfloor \log_2\left(\frac{n}{2}\right) \right\rfloor$$

where n is the number of data points in the signal (equally spaced) and $\lfloor x \rfloor$ is the floor to x , that is, the largest integer smaller than x . Thus for

$n = 240$, $n_{oct} = 6$. If n is the number of data points for gold or chlorite along a drill hole n meters long then n is expressed in meters.

The smallest wavelet scale, α_{scale} , for the Mexican hat mother wavelet is given by

$$\alpha_{scale} = \left[\left(2\pi\sqrt{\frac{2}{5}} \right) \sigma \right]^{-1}$$

where σ is the width of the hat, taken to be equal to one so that $\alpha_{scale} = 0.25165$ units. The units correspond to those used to measure the distance between points. The scaling parameter for a particular octave and voice is given by

$$s_{octave,voice} = \alpha_{scale} 2^{octave-1} 2^{voice/n_{voice}}$$

where, in Mathematica®, n_{voice} is taken to be 4 so that

$$s_{1,1} = 0.25165 \times 2^{1-1} 2^{1/4} = 0.299359$$

and each successive voice differs from the one smaller by a factor of $2^{1/4}$ or 1.19.

Thus, if the signal consists of 240 points each 1 m apart, $n_{oct} = 6$ and the array (Eq. (B.1)) becomes

[0.299359], [0.355881], [0.423217], [0.503292]	octave 1, voices 1 to 4
[0.598519], [0.711763], [0.846433], [1.00658]	octave 2, voices 5 to 8
[1.19704], [1.42353], [1.69287], [2.01317]	octave 3, voices 9 to 12
[2.39407], [2.84705], [3.38574], [4.02634]	octave 4, voices 13 to 16
[4.78815], [5.6941], [6.77146], [8.05267]	octave 5, voices 17 to 20
[9.5763], [11.3882], [13.5429], [16.1053]	octave 6, voices 21 to 24

(B.2)

In this case, the voices, in square brackets, are expressed in meters.

The vertical axis on the scalogram can be represented by the array (Eq. (B.1)) or as Eq. (B.2) or more simply by just the octaves, numbered 1 to n_{oct} . In this paper we use only the octaves but to convert scales to meters, as in the Hurst exponent measurements, the above discussion is relevant.

In exploring multifractal geometries it is convenient to define the generalised fractal dimension, D_q , which is related to the scaling exponent for the q th moment of the measure μ . If we have a set of measures, say the concentration of a chemical component such as Na distributed over a fabric, we define the q th moment (or partition function) $\mathbb{Z}(q, \varepsilon)$ for the box size ε as (Lynch, 2007):

$$\mathbb{Z}(q, \varepsilon) = \sum_{i=1}^{N(\varepsilon)} \mu_i^q (\varepsilon) \quad (\text{B.3})$$

Then we can also define $\tau(q)$ as

$$\tau(q) = \lim_{\varepsilon \rightarrow 0} \frac{\ln \mathbb{Z}(q, \varepsilon)}{-\ln \varepsilon} \quad (\text{B.4})$$

The generalised fractal dimensions D_q are given by:

$$\tau(q) = D_q(1-q) \quad (\text{B.5})$$

In the limit $\varepsilon \rightarrow 0^+$, $\mathbb{Z}(q, \varepsilon)$ behaves as a power law:

$$\mathbb{Z}(q, \varepsilon) \sim \varepsilon^{-\tau(q)} \quad (\text{B.6})$$

The relations between the $f(\alpha)$ singularity spectrum, q and the $\tau(q) = (1-q)D_q$ spectrum are given (Arneodo et al., 1995) by:

$$q = \frac{df(\alpha)}{d\alpha}$$

$$\frac{d^2 f(\alpha)}{d\alpha^2} < 0$$

$$\tau(q) = q\alpha - f(\alpha).$$

A discussion of the WTMM formalism is given in Hobbs and Ord (2015, pp 235–239).

References

- Agterberg, F.P., 1995. Multifractal modelling of the sizes and grades of giant and supergiant deposits. *Int. Geol. Rev.* 37, 1–8.
- Agterberg, F.P., 2007. Mixtures of multiplicative cascade models in geochemistry. *Nonlinear Process. Geophys.* 14, 201–209.
- Agterberg, F.P., 2012. Sampling and analysis of chemical element concentration distribution in rock units and orebodies. *Nonlinear Process. Geophys.* 19, 23–44.
- Arias, M., Gumieli, P., Sanderson, D.J., Martin-Izard, A., 2011. A multifractal simulation model for the distribution of VMS deposits in the Spanish segment of the Iberian Pyrite Belt. *Comput. Geosci.* 37, 1917–1927.
- Aris, R., 1961. *The Optimal Design of Chemical Reactors*. Elsevier.
- Aris, R., 1978. *Mathematical Modelling Techniques*. Research Notes in Mathematics. 24 Piman.
- Aris, R., 1999. On some dynamical diagrams of chemical reaction engineering. *Chaos* 9, 3–12.
- Arneodo, A., Audit, B., Decoster, N., Muzy, J.-F., Vaillant, C., 2002. Wavelet based multifractal formalism: applications to DNA sequences, satellite images of cloud structure and stock market data. In: Bunde, A., Kropp, A., Schellnhuber, H.J. (Eds.), *The Science of Disasters: Climate Disruptions, Heart Attacks and Market Crashes*. Springer, pp. 26–102.
- Arneodo, A., Audit, B., Kestener, P., Roux, S., 2003. A wavelet-based method for multifractal image analysis: from theoretical concepts to experimental applications. In: Hawkes, P.W. (Ed.), *Advances in Imaging and Electron Physics*. 126, pp. 1–92.
- Arneodo, A., Bacry, E., Muzy, J.F., 1995. The thermodynamics of fractals revisited with wavelets. *Physica A* 213, 232–275.
- Arneodo, A., Grasseau, G., Kostelich, E.J., 1987. Fractal dimensions and $f(\alpha)$ spectrum of the Henon attractor. *Phys. Lett. A* 124, 426–432.
- Bak, P., 1996. *How Nature Works: The Science of Self-organized Criticality*. Copernicus, Springer-Verlag, New York.
- Bak, P., Tang, C., Wiesenfeld, K., 1987. Self-organised criticality. An explanation of 1/f noise. *Phys. Rev. Lett.* 59, 381–384.
- Baldyga, J., Pohorecki, R., 1995. Turbulent micromixing in chemical reactors—a review. *The Chemical Engineering Journal and the Biochemical Engineering Journal* 58, 183–195.
- Bastrakov, E.N., Skirrow, R.G., Didson, G.J., 2007. Fluid evolution and origins of iron oxide Cu-Au prospects in the Olympic Dam district, Gawler craton, South Australia. *Econ. Geol.* 102, 1415–1440.
- Beck, C., Schlögl, F., 1993. *Thermodynamics of Chaotic Systems*. Cambridge University Press.
- Bejan, A., Lorente, S., 2008. *Design with Constructal Theory*. Wiley.
- Berezowski, M., 2000. Spatio-temporal chaos in tubular chemical reactors with the recycle of mass. *Chaos, Solitons Fractals* 11, 1197–1204.
- Berezowski, M., 2014. *Fractals, Bifurcations and Chaos in Chemical Reactors*. Lap Lambert Academic Publishing.
- Berezowski, M., Ptaszek, P., Jacobsen, E.W., 2000. Dynamics of heat-integrated pseudohomogeneous tubular reactors with axial dispersion. *Chem. Eng. Process.* 39, 181–188.
- Blenkinsop, T.G., Doyle, M.G., 2014. Structural controls on gold mineralization on the margin of the Yilgarn craton, Albany-Fraser orogen: the Tropicana deposit, Western Australia. *J. Struct. Geol.* 67, 189–204.
- Bohr, T., Tel, T., 1988. The thermodynamics of fractals. In: Hao, B.-L. (Ed.), *Directions in Chaos*. World Scientific, Singapore, pp. 194–237.
- Burghardt, A., Berezowski, M., 1996. Analysis of the bifurcation of oscillatory solutions in a porous catalytic pellet: influence of the reaction order. *Chem. Eng. Sci.* 51, 3307–3316.
- Carlson, C.A., 1991. Spatial distribution of ore deposits. *Geology* 19, 111–114.
- Chainais, P., 2006. Multidimensional infinitely divisible cascades. *The European Physical Journal B* 51, 229–243.
- Cheng, Q., Cheng, Q., 2008. GIS based fractal and multifractal methods for mineral deposit prediction. In: Bonham-Carter, G. (Ed.), *Nonlinear Theory and Power-law Models for Information Integration and Mineral Resources Quantitative Assessments*. Progress in Geomatics. Springer, pp. 185–225.
- Cheng, Q., Agterberg, F.P., 1996. Multifractal modelling and spatial statistics. *Math. Geol.* 28, 1–16.
- Chhabra, A., Jensen, R.V., 1989. Direct determination of the $f(\alpha)$ singularity spectrum. *Phys. Rev. Lett.* 62, 1327–1330.
- Cross, M., Greenside, H., 2009. *Pattern Formation and Dynamics in Nonequilibrium Systems*. Cambridge University Press.
- de Wijs, H.J., 1951. Statistics of ore distribution. Part 1: frequency distribution of assay values. *Geol. Mijnb.* 13, 365–375.
- de Wijs, H.J., 1953. Statistics of ore distribution. Part 2: theory of binomial distribution applied to sampling and engineering problems. *Geol. Mijnb.* 15, 12–24.
- Drazin, P.G., Reid, W.H., 1981. *Hydrodynamic Stability*. Cambridge University Press, Cambridge, UK.
- Drozdz, S., Oswiecimka, P., 2015. Detecting and interpreting distortions in hierarchical organization of complex time series. *Phys. Rev. E* 91, 030902(R).
- Epstein, I.R., Pojman, J.A., 1998. *An Introduction to Nonlinear Chemical Dynamics*. Oxford University Press.
- Faghfouri, A., 2011. *Multifractal Analysis and Modelling of Lightning Stroke Maps for Power Systems* PhD thesis University of Manitoba.
- Feder, J., 1988. *Fractals*. Plenum, New York.
- Felder, R.M., Hill, F.B., 1969. Mixing effects in chemical reactors. I. Reactant mixing in batch and flow systems. *Chem. Eng. Sci.* 24, 385–398.
- Ford, A., Blenkinsop, T.G., 2009. An expanded de Wijs model for multifractal analysis of mineral production data. *Mineral. Deposita* 44, 233–240.
- Frisch, U., 1995. *Turbulence*. Cambridge University Press.
- Gibbs, J.W., 1902. *Elementary Principles in Statistical Mechanics*. Yale University Press Dover rendition, 1960.
- Gonzalez, C.M., Gorczyk, W., Gerya, T.V., 2015. Decarbonation of subducting slabs: Insight from petrological-thermomechanical modeling. *Gondwana Res.* <http://dx.doi.org/10.1016/j.gr.2015.07.011>.
- Gou, X.-Q., Zhang, Y.-J., Dong, W.-S., Qie, X.-S., 2007. Wavelet-based multifractal analysis of the radiation field of first return stroke in cloud-to-ground discharge. *Chin. J. Geophys.* 50, 104–109.
- Gray, P., Scott, S.K., 1994. *Chemical Oscillations and Instabilities*. Clarendon Press, Oxford.
- Hill, J.E., Oliver, N.H.S., Cleverley, J.S., Nugus, M.J., Carswell, J., Clark, F., 2014. Characterisation and 3D modelling of a nuggety, vein-hosted gold ore body, Sunrise Dam, Western Australia. *J. Struct. Geol.* 67, 222–234.
- Hobbs, B.E., Ord, A., 2015. *Structural Geology: The Mechanics of Deforming Metamorphic Rocks*. Elsevier.
- Hodkiewicz, P.F., Weinberg, R.F., Gardoll, S.J., Groves, D.I., 2005. Complexity gradients in the Yilgarn Craton: fundamental controls on crustal-scale fluid flow and the formation of world-class orogenic-gold deposits. *Aust. J. Earth Sci.* 52, 831–841.
- Hunt, J.A., Baker, T., Thorkelson, D.J., 2007. A review of iron oxide copper-gold deposits, with focus on the Wernecke Breccias, Yukon, Canada, as an example of a non-magmatic end member and implications for IOCG genesis and classification. *Explor. Min. Geol.* 16, 209–232.
- Ihlen, E.A.F., 2012. Introduction to multifractal detrending fluctuation analysis in MATLAB. *Front. Physiol.* 3, 1–18.
- Ihlen, E.A.F., Vereijken, B., 2010. Interactive-dominant dynamics in human cognition: beyond $1/f^\alpha$ fluctuation. *J. Exp. Psychol. Gen.* 119, 436–463.
- Kahler, C., Rossler, O.E., Varma, A., 1981. Chaos in continuous stirred tank reactor with two consecutive first-order reactions, one exo-, one endothermic. In: Ebert, W.H., Deufhard, P., Jager, W. (Eds.), *Modelling of Chemical Reaction Systems*. Springer-Verlag, pp. 355–365.
- Kestener, P., Arneodo, A., 2003. Three-dimensional wavelet-based multifractal method: the need for revisiting the multifractal description of turbulence dissipation data. *Phys. Rev. Lett.* 91, 194501.
- Kruhl, J.H., 1994. The formation of extensional veins: an application of the Cantor-dust model. In: Kruhl, J.H. (Ed.), *Fractals and Dynamic Systems in Geoscience*. Springer-Verlag, Berlin, pp. 95–104.
- Kruhl, J.H., 2013. Fractal-geometry techniques in the quantification of complex rock structures: a special view on scaling regimes, inhomogeneity and anisotropy. *J. Struct. Geol.* 46, 2–21.
- Lester, D.R., Ord, A., Hobbs, B.E., 2012. The mechanics of hydrothermal systems: II. Fluid mixing and chemical reactions. *Ore Geol. Rev.* 49, 45–71.
- Li, W., Jun, D., Qingfei, W., 2009. Multifractal modeling and evaluation of inhomogeneity of metallogenic elements distribution in the Shangzhuang Deposit, Shandong Province, China. *Computational Intelligence and Software Engineering (CISE). International Conference* 4 pp.
- Liu, H., Wang, Q., Li, G., Wan, L., 2012. Characterization of multi-type mineralizations in the Wandangshan gold poly-metallic deposit, Yunnan (China), by fractal analysis. *J. Geochim. Explor.* 122, 20–33.
- Lockner, D.A., Byerlee, J., 1980. Development of fracture planes during creep in granite. In: Hardy, H.R., Leighton, F.W. (Eds.), *2nd Conference on Acoustic Emission/Microseismic Activity in Geological Structures and Materials*. Trans-Tech. Publications, Clausthal-Zellerfeld, pp. 11–25.
- Lorenz, E.N., 1963. Deterministic nonperiodic flow. *J. Atmos. Sci.* 20, 130–141.
- Lotka, A.J., 1910. Contribution to the theory of periodic reactions. *J. Phys. Chem.* 14, 271–274.
- Lotka, A.J., 1920. Undamped oscillations derived from the law of mass action. *J. Am. Chem. Soc.* 42, 1595–1599.
- Lundin, E.R., 2013. Plumes do that. In: Hall, M. (ed.), *52 Things You Should Know About Geology*. Agile Libre, 66–67.
- Lyakhovsky, V., Ben-Zion, Y., 2008. Scaling relations of earthquakes and aseismic deformation in a damage rheology model. *Geophys. J. Int.* 172, 651–662.
- Lyakhovsky, V., Hamiel, Y., Ben-Zion, Y., 2011. A non-local visco-elastic damage model and dynamic fracturing. *Journal of Mechanics and Physics of Solids* 59, 1752–1776.
- Lynch, S., 2007. *Dynamical Systems with Applications using Mathematica®*. Birkhäuser.
- Lynch, D.T., Rogers, T.D., Wanke, S.E., 1982. Chaos in a continuously stirred tank reactor. *Mathematical Modelling* 3, 103–116.
- Mandelbrot, B., 1974. Intermittent turbulence in self-similar cascades: divergence of high moments and dimensions of the carrier. *J. Fluid Mech.* 62, 331–358.
- Mandelbrot, B., 1982. *The Fractal Geometry of Nature*. W.H. Freeman & Co.
- Mandelbrot, B., Evertsz, C.J.G., 1991. Exactly self-similar left-sided multifractals. In: Bunde, A., et al. (Eds.), *Fractals and Disordered Systems*. Springer-Verlag, pp. 323–344.
- Munro, M., Ord, A., Hobbs, B.E., 2016. Multifractal singularity spectra: The DNA of Archaeal hydrothermal Au systems. Submitted to *Ore Geology Reviews*.

- Newman, M.E.J., 2006. Power laws, Pareto distributions and Zipf's law. *Contemp. Phys.* 46, 323–351.
- Occhipinti, S.A., Metelka, V., Lindsay, M.D., Hollis, J.A., Aitken, A.R.A., Tyler, I.M., Miller, J.M., McCuaig, T.C., 2016. Multicommodity mineral systems analysis highlighting mineral prospectivity in the Halls Creek Orogen. *Ore Geol. Rev.* 72, 86–113.
- Onsager, L., 1944. Crystal Statistics. I. A two-dimensional model with an order-disorder transition. *Phys. Rev.* 65, 117–149.
- Ord, A., Hobbs, B.E., Lester, D.R., 2012. The mechanics of hydrothermal systems: I. Ore systems as chemical reactors. *Ore Geol. Rev.* 49, 1–44.
- Oreskes, N., Einaudi, M.T., 1990. Origin of rare earth element-enriched hematite breccias at the Olympic Dam Cu-U-Au-Ag deposit, Roxby Downs, South Australia. *Econ. Geol.* 85, 1–28.
- Ottino, J.M., 1994. Mixing and chemical reactions. A tutorial. *Chemical Engineering Science* 49, 4005–4027.
- Poincaré, H., 1892. *Les Méthodes Nouvelles de la Mécanique Celeste*. Gauthier-Villars, Paris.
- Prigogine, I., 1955. *Introduction to Thermodynamics of Irreversible Processes*. Wiley.
- Qingfei, W., Jun, D., Li, W.A.N., Jie, Z., Qingjie, G., Liqiang, Y., Lei, Z., Zhijun, Z., 2008. Multifractal analysis of element distribution in skarn-type deposits in the Shizishan Orefield, Tongling Area, Anhui Province, China. *Acta Geologica Sinica - English Edition* 82, 896–905.
- Richardson, L.F., 1922. *Weather Prediction by Numerical Process*. Cambridge University Press.
- Riedi, R.H., 1998. Multifractals and wavelets: a potential tool in geophysics. Proceedings of the 68th Annual International Meeting of the Society of Exploration Geophysicists. Society of Exploration Geophysicists, New Orleans, LA 4 pp.
- Ross, J., 2008. *Thermodynamics and Fluctuations Far From Equilibrium*. Springer-Verlag.
- Rudnicki, J.W., Rice, J.R., 1975. Conditions for the localization of deformation in pressure-sensitive dilatant materials. *Journal of the Mechanics and Physics of Solids* 23, 371–394.
- Sanderson, D.J., Roberts, S., Gumieli, P., Greenfield, C., 2008. Quantitative analysis of tin- and tungsten-bearing sheeted vein systems. *Econ. Geol.* 103, 1043–1056.
- Schodde, R.C., Hronsky, J.M.A., 2006. The role of world-class mines in wealth creation. In: Doggett, M.D., Parry, J.R. (Eds.), *Wealth Creation in the Minerals Industry: Integrating Science, Business, and Education* vol. 12. Society of Economic Geologists Special Publications Series, pp. 71–90.
- Schroeder, M., 1991. *Fractals, Chaos, Power Laws*. W.H. Freeman, New York.
- Sethna, J.P., 2011. *Statistical Mechanics. Entropy, Order Parameters and Complexity*. Clarendon Press, Oxford.
- Sornette, D., 2006. *Critical Phenomena in Natural Sciences; Chaos, Fractals, Self-Organization and Disorder: Concepts and Tools*. Springer-Verlag, Berlin.
- Sprott, J.C., 2003. *Chaos and Time-series Analysis*. Oxford University Press, Oxford.
- Sun, T., Liu, L., 2014. Delineating the complexity of Cu-Mo mineralisation in a porphyry copper intrusion by computational and fractal modelling: a case study of the Chehugou deposit in the Chifeng district, Inner Mongolia, China. *J. Geochem. Explor.* 144, 128–143.
- Tang, X.Z., Boozer, A.H., 1999. Design criteria of a chemical reactor based on a chaotic flow. *Chaos* 9, 183–194.
- Turcotte, D.L., 1986. A fractal approach to the relationship between ore grade and tonnage. *Econ. Geol.* 81, 1528–1532.
- Villermaux, J., 1986. Macro and micromixing phenomena in chemical reactions. In: de Lasas, H.I. (Ed.), *Chemical Reactor Design and Technology*. Martinus Nijhoff Publishers, pp. 191–244.
- Weinstein, H., Adler, R.J., 1967. Micromixing effects in continuous chemical reactors. *Chem. Eng. Sci.* 65–75.
- Zapperi, S., Backard, K., Stanley, H.E., 1995. Self-organized branching processes: mean-field theory for avalanches. *Phys. Rev. Lett.* 75, 4071–4074.
- Zhao, C., Hobbs, B.E., Ord, A., 2008. *Convective and Advective Heat Transfer in Geological Systems*. Springer.
- Zhao, C., Hobbs, B.E., Ord, A., 2009. *Fundamentals of Computational Geoscience*. Springer.